IEEE Access
Multidisciplinary | Rapid Review | Open Access Journal

IEEE PHOTONICS SOCIETY SECTION

Received December 15, 2021, accepted January 13, 2022, date of publication January 18, 2022, date of current version January 27, 2022.

Digital Object Identifier 10.1109/ACCESS.2022.3144330

Towards InAs/InP Quantum-Dash Laser-Based Ultra-High Capacity Heterogeneous Optical Networks: A Review

MOHAMMED ZAHED MUSTAFA KHAN, (Senior Member, IEEE)
Optoelectronics Research Laboratory, Electrical Engineering Department, King Fahd University of Petroleum and Minerals, Dhahran 31261, Saudi Arabia
Center for Communication Systems and Sensing, King Fahd University of Petroleum and Minerals, Dhahran 31261, Saudi Arabia

e-mail: zahedmk@kfupm.edu.sa

This work was supported by the Deanship of Research Oversight and Coordination (DROC) at King Fahd University of Petroleum and Minerals through the Research Center for Communication Systems and Sensing under Grant SB201008.

ABSTRACT The unprecedented increase in internet traffic witnessed in the last few years has pushed the community to explore heterogeneous optical networks, including free-space-optics (FSO) communication, radio-over-fiber (RoF), wireless (WL), and their convergent hybrid technologies. This stems from the possibility of seamless integration with the existing fiber-optic backhaul networks while providing much-needed flexibility and scalability. Moreover, efficient optical transceivers, particularly light sources in the form of semiconductor laser diodes, are key in meeting the future demands of the next generation green optical access networks. In this respect, InAs/InP Quantum-dash (Qdash) nanostructure-based lasers have shown tremendous progress in the past few years with applications spanning from a wavelength division multiplexed (WDM) optical communication to recently, millimeter-wave (MMW) over fiber networks. This waveguide-based laser diode (LD) has demonstrated a rule-changing broad multi-wavelength lasing emission, thanks to the inherent and wavelength-tunable wide gain profile offered by the Qdash active-gain region covering S- to U-band regions. Moreover, exploiting mode-locking and optical injection locking assisting techniques, highly coherent InAs/InP Qdash comb laser source at 1550 nm and 1610 nm have been respectively realized, thus opening a new paradigm for their potential applications in green optical and 5G access networks. In this work, progress on utilizing InAs/InP Qdash LD, supporting several sub-carriers, in energy-efficient $\sim$1550 nm and $\sim$1610 nm WDM heterogeneous optical networks with single-mode-fibers (SMF) has been highlighted, exhibiting aggregate data rates of 11 – 12 Tb/s by employing a single device, and accommodating PAM4 and higher-order 32-QAM modulation schemes. Moreover, the recent deployment of this LD in the RoF domain, targeting MMW frequency band, for convergent fiber-wireless networks, is also summarized, with demonstrated 25 to >100 GHz MMW beat-tone frequency generates and transmission of up to 24 Gb/s.

INDEX TERMS Quantum-dash/dot lasers, semiconductor lasers, mode-locking, injection-locking, wavelength division multiplexing, millimeter waves, free-space optical communication, radio-over-fiber.

I. INTRODUCTION

The need for high bandwidth optical communication networks is intensifying due to the sharp increase in the number of end-users and their demand for high-speed mobile and internet connectivity. Internet traffic is witnessing rapid growth in requirements and system capacities due to the explosive demand of consumer applications such as Ultra-High-Definition Television and streaming, Voice over Internet Protocol (VoIP), and Internet of Things (IoT). In the foreseeable future, current technologies will struggle to keep up with the ever-growing internet traffic demand [1], [2]. It is estimated that nearly one-third of the global population will have internet access by 2023, with 5.3 billion total internet users, up from 3.9 billion in 2018 [3]. Moreover, it is also projected that the internet data traffic will reach 270 Exabytes per month by 2021, while the annual traffic will reach almost 2.3 Zettabytes (1ZB $= 10^{21}$B) [4]. Thus, it becomes paramount to develop optical telecommunication paradigms to satisfy the markets, industries, and consumer demands.

A passive optical network (PON) is an access-layer optical-fiber network that utilizes a point-to-multipoint topology with

The associate editor coordinating the review of this manuscript and approving it for publication was Leo Spiekman.

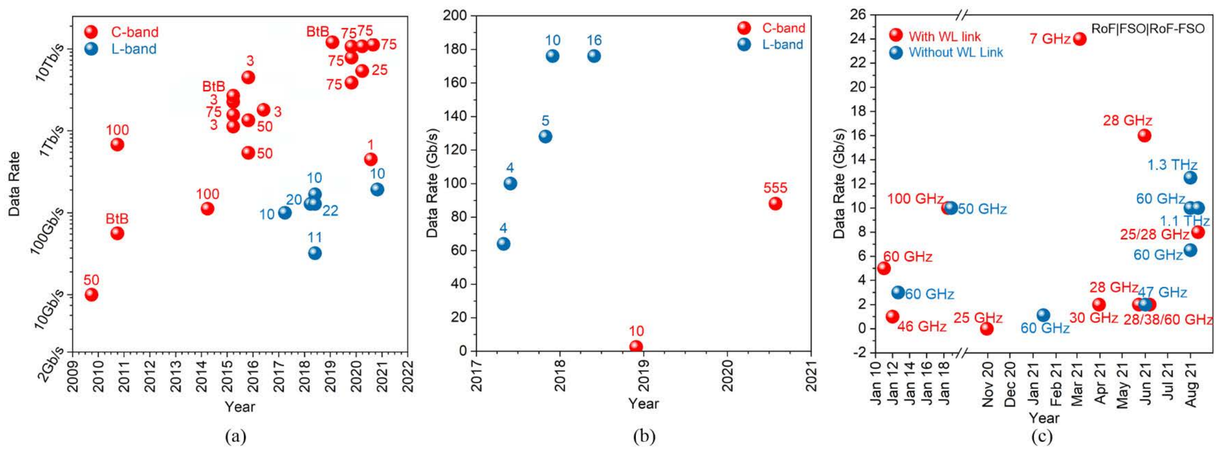

FIGURE 1. Summary of the demonstrated aggregate data rates achieved over (a) SMF, (b) FSO, and (c) MMW/THz wave optical communication incorporating InAs/InP Qdash LD as optical sources in literature, which are referenced at the end of this review work. The labels in (a) shows the SMF length in km, while (b) shows the length of the FSO link in meters. The labels in (c) show the corresponding generated MMW beat-tone frequency.

the aid of passive optical splitters to transmit the data from a single point, an Optical Line Terminal (OLT), to multiple user-points, Optical Network Units (ONUs). In PONs, the upstream and downstream signals are transmitted simultaneously in both directions. The passive nature of these networks is ascribed to the un-powered nature of the channel (the optical fiber) and the splitting/combining components, in addition to not requiring active cooling nor continuous maintenance, allowing them to last for decades if kept undisturbed [2], which all drastically reduces the operation expenditure (OpEx). PONs have evolved into 10G Passive Optical Network (XG-PON) in addition to the so-called Next-Generation Passive Optical Networks (NG-PONs), which is planned to take place in the form of three stages, NG-PON1, NG-PON2, and NG-PON3, all sharing the primary target of maximizing the per-user capacity and increasing the number of possible subscribers, in addition to expanding the network range [5].

Furthermore, contrary to NG-PON1 and XG-PON, future NG-PONs are not envisioned to be restricted by backward-compatibility requirements, which would allow for myriad novel and innovative paradigms and architectures with unique new features. Similarly, fully adaptive bandwidth-allocation to the subscribers and the fine wavelength tunability have been identified as equally desirable features. As such, the NG-PONs would flexibly accommodate newly emerging services and applications. Lastly, future NG-PONs need to be a green form of communication in addition to being cost-efficient in terms of capital expenditure (CapEx) and OpEx to remain attractive and practical given their limited range (<100 km) when compared to long-haul fiber-optic networks whose distance-bandwidth products are sufficiently large to justify their high implementation costs [6].

To keep up with the roadmap and evolution of the NG-PON infrastructures, effective semiconductor optoelectronics devices, mainly light sources, need to be investigated in these architectures. To that end, Qdash nanostructure-based semiconductor laser diodes are very attractive solutions due to their advantages such as compact size, low power consumption, fabrication simplicity, and integrability in hybrid optical-silicon systems [7], [8]. More significantly, due to their broadband density of state/gain profiles, they emit ultra-broad bandwidths with emissions covering the S-, C-, L-, and U-bands. Potentially, the broadband nature of Qdash laser sources could be exploited in two different aspects. Firstly, the broadband Qdash source may well be utilized as a singular light source that can provide several wavelengths, one for each channel, instead of several narrow-band sources, in a multi-wavelength network. Secondly, broadband Qdash lasers may possibly be used as a unified colorless transmitter at each OLT/ONU in injection-locked PONs, allowing for mass deployment making it much more convenient, and time- and cost-effective when compared to deployment of non-identical sources, thus cutting the CapEx drastically and allows for seamless scalability.

One of the most promising approaches to realize the NG-PONs' primary requirements of maximizing the per-user capacity and increasing the number of possible subscribers is unrestricting the utilizable bandwidth to the well-exhausted and saturated C-band exclusively and instead of extending it to the neighboring L-band, as a natural evolution [1]. To that end, L-band Qdash LDs stand out as prime candidates whose broadband gain profiles and lasing emission bandwidths have been exploited to realize multi-wavelength or comb sources thanks to their inhomogeneous sizes due to the random nature of the self-assembly growth process. Consequently, this has qualified them as ideal contenders for source-unified NG-PON paradigms [9].

The exponential rise of smart devices has substantially increased the demand for mobile data traffic. Fifth-generation new radio wireless (WL) mobile networks have been developed to meet this demand by providing ultra-reliable and low latency communications, enhanced mobile broadband, ultra-fast data transfer, and support applications such as high-definition video streaming, autonomous driving, teleconferencing, internet of things [10]. According to 5G Public-Private Partnership, future 5G WL technology is expected to provide subscribers with data rates of Gigabits per second while using the MMW frequency spectrum from 20 to 30 GHz [11], since below 6 GHz window is already congested by the WL services [12]. Although MMW suffers from significant signal fading due to high atmospheric attenuation, its seamless integration with existing fiber-to-the-x (FTTX) architecture for last-mile access allows for delivering ultra-broadband WL signals at the user-end well-known as RoF technology. Furthermore, hybrid RoF and WL technologies are being considered as potential frontiers for next-generation networks.

This review provides a complete walk-through of the different demonstrations of optical communications systems in literature employing Qdash LDs as optical sources and summarizes the progress over the years of the achieved transmission capacity in Fig. 1. Firstly, a brief background about Qdash materials and their broadband nature is given in section II. Then, section III discusses Qdash laser devices and some of the key concepts and techniques incorporated in their design and operation. Afterward, section IV discusses the optical-fiber-based transmission demonstrations with Qdash LDs as light sources and are categorized according to their wavelength emission either in the C-band or in L-band, whose summary is provided in Fig. 1(a). Then, section V explores free-space-optics (FSO) communication, another frontier for NGPONs, providing seamless integration of rural areas and regions where fiber deployment is difficult with the existing optical networks. In this section, reports from literature incorporating deployment of Qdash LDs in indoor and outdoor FSO channels are discussed and shown in Fig. 1(b). Lastly, section VI overviews the implementation of Qdash lasers as a means of photonic generation of MMW and terahertz (THz) wave and their transmission demonstrations, with the progress illustrated in Fig. 1(c).

II. BACKGROUND

In literature, system-level and device-level approaches have been explored to expand the data transmission capacity of optical communication networks and break the Tb/s barrier. The first methodology investigates techniques to improve encoding a signal and its transmission environment wherein sophisticated modulation/ demodulation techniques are developed for a given bandwidth. Furthermore, developing multiplexed network architectures exploiting signal's wavelength/time/frequency/polarization or utilizing physical infrastructures such as space-division multiplexing in the form of novel multi-core and few-mode fibers, FSO, etc., have also been considered [13].

On the other hand, the device-level direction investigates the optical network's fundamental elements: transmitters and receivers. Developing efficient and high-performance active optoelectronic devices such as light sources, photodiodes, optical amplifiers, and modulators are equally paramount in attaining Tb/s data capacity network [13]. Hence, this review summarizes the recent progress in developing efficient light sources in the form of the quantum-confined active region-based semiconductor LDs and their deployment in optical communication to achieve beyond Tb/s data capacity, thus evolving as a candidate light source for green communication NG-PONs. In the subsequent sections, an introduction to quantum-dash nanostructures has been provided, highlighting its niche features that have been exploited in the remarkable improvement of optical communication network's data capacity.

A. QUANTUM DASH NANOSTRUCTURES

Typically, Quantum-well (Qwell) nanostructures confine the quasiparticles along one dimension. On the other hand, two- and three-dimensional confinement is attainable in quantum-wire (Qwires) and quantum-dots (Qdots) nanostructures, respectively. At a quantum-length scale, the 3D-confinement to discrete energy levels is analogous to the textbook case of a particle-in-a-box (in contrast to the particle-in-a-well in the case of Qwells). This high degree of confinement leads to a more carrier-localization resulting in a complete breakdown of the band structure and atom-like properties with size- and confinement-dependent energy levels. These properties have been exploited in literature to realize high-performance light emitters and detectors, thereby significantly improving the data transmission capacity. In traditional epitaxial techniques to grow these light emitter/detector device structures, the growth process is carried out by depositing crystalline over-layers on a substrate layer in a layer-by-layer fashion where each layer is lattice-matched with the subsequent layers. This results in uniform and highly crystalline two-dimensional layers, which is the case in double heterostructure (DHS) and Qwells. These techniques have long required careful lattice matching between the substrate layer and the subsequently grown over-layers to eliminate strain-mismatch occurrence between these layers that would otherwise result in defects and dislocations that are detrimental to the electron-hole pair recombination rates and carrier mobility within the active medium [14].

On the other hand, Qwires and Qdots are produced through different growth techniques. The most common among said techniques is the Stranski-Krastanov (S-K) growth mode [15]. In this technique, a deliberate lattice-mismatch is introduced in between the layers ($4 - 7\%$ for InAs/GaAs and InAs/InP) by depositing materials of large lattice constants (*e.g.,* InAs) over a material of a smaller lattice constant (*e.g.,* GaAs). Initially, surface-energetics favor a planar growth of the deposited layers resulting in a 2D barrier layer. However, as the thickness increases with the deposition of more materials, the surface-energy is counter-balanced by the built-up strain-energy due to mismatched lattice constants, which results in the reorganization of the Qdot (Qwire) material, spontaneously, into 3D- (2D-) islands within thin 2D layers (wetting layers) in a self-assembly process allowing for a more efficient strain-relaxation [16]. Afterward, a lattice-matched material is deposited over the grown islands and

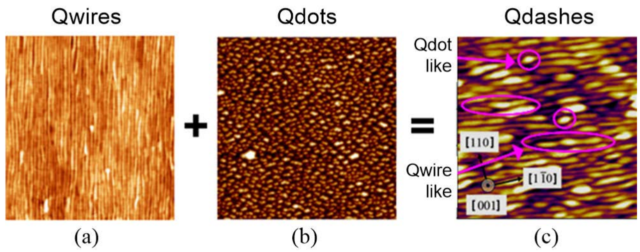

FIGURE 2. AFM micrographs of (a) Qwires [18], (b) Qdots [19], and (c) Qdashes [22].

completes the confinement potential, while the lattice constant adapts to the overgrowing material for the growth of the subsequent layers smoothly and defect-free [17]. A proper strain engineering approach is required to grow either Qdots or Qwires, whose atomic force microscope (AFM) sample planar views are shown in Figs. 2(a) and (b), respectively [18], [19]. As seen, the naturally occurring shape- and size-fluctuations in the grown Qdots and Qwires are clearly visible in the form of the variations in the brightness of the grown islands within the AFM micrographs.

Different material systems can be incorporated with the S-K growth mode technique. Nevertheless, when growing thin InAs layers over an InP(100) platform, to realize laser diodes in the C-band region, a relatively small lattice mismatch (3.2%) takes place between the grown layers, which results in a reduced isotropic strain along one direction (*viz.*, [1 −1 0]). In addition to other growth kinetics, this anisotropic surface strain dominates the self-assembly process, resulting in the formation of elongated nanostructures along the same direction (Fig. 2(c)), instead of 3D Qdot islands as is the case with other material systems. These unique asymmetric nanostructures resemble a hybrid structure between Qwires and Qdots, which are commonly known as Qdash structures that possess intermediate properties between Qwells and Qdots. The dimensions of these elongated Qdashes, *i.e.*, width, height, and length, are generally in the range of ∼10 − 20 nm, ∼1 − 4 nm, and ∼30 to hundreds of nm, respectively [20]. Unlike zero-dimensional confinement of carriers in Qdots, only two dimensions exhibit quantum confinement leaving the elongation direction unconfined, thus limiting the Qdashes' carrier confinement. This, in turn, prevents the structure from exploiting the full benefits of a true-zero-dimensional density of states (DoS) and instead results in a quasi-zero-dimensional DoS and hence, behaves like and acquires the electronic and optical properties of Qwires [21]. These low-dimensional nanostructures have attracted the attention of research and investigation since their inception in 1996 due to their emission at longer wavelengths. Moreover, since Qdashes exhibit more material coverage due to large volume, compared to Qdots, they tend to achieve higher material and modal gain [20].

B. INHOMOGENEOUS BROADENING

Generally, the electron-hole transition energies within each Qdot/Qdash depend on its geometrical dimensions, where smaller Qdots/Qdashes (particularly in terms of height) are associated with wider transition energy hence, emit at shorter wavelengths of light. The self-assembly process in the S-K growth technique is a stochastic process that results in Qdots/Qdashes that vary the size, distance, shape, and composition, as indicated by the brightness fluctuations in the AFM micrographs of Fig. 2(c) [22]. This random process could only be controlled by macroscopic parameters, such as substrate temperature, growth rate, etc. Consequently, this results in dissimilar confinement potentials among each Qdot/Qdash, and thereby, the description of true-zero-dimensional/quasi-zero-dimensional DoS is no longer valid while the concept of ensembles has been used instead. An ensemble of Qdots/Qdashes assumes a group of similar Qdots/Qdashes, usually within a single layer/stack, with a single ground state (GS) band-transition energy (E_0) taking a Lorentzian-like homogeneous broadening profile with a width Γ_{hom} and energy variations across dash groups resulting in a shared Gaussian-like inhomogeneously broadened DoS/gain envelope. Fig. 3(a) shows an example of a less inhomogeneously broadened DoS/gain profile of a Qdot/Qdash ensemble, while Fig. 3(b) illustrates a broadened DoS/gain profile with the Gaussian envelope width Γ_{inh} indicating the GS interband transition energy spread of the Qdots/Qdash ensembles and qualitatively dictates the gain profile of the whole active region [23]. These different energy transitions have been exploited to collectively attain a broad gain profile for realizing broadband lasers. Furthermore, bandgap engineering during the growth process, known as chirping the active region, can be incorporated to further increase the inhomogeneous broadening by varying the strain during the growth of the different Qdot/Qdash layers/stacks by varying the barrier/capping layer thickness/composition, or by modifying the material composition of the Qdots/Qdashes

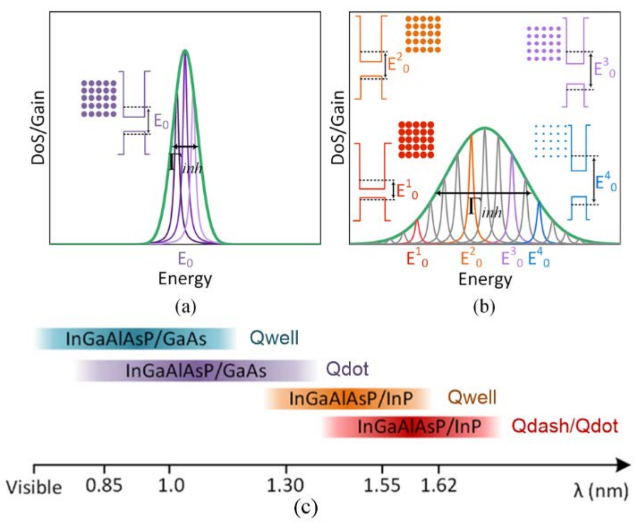

FIGURE 3. Representation of (a) less inhomogeneous system with narrow Gaussian DoS/gain profile of Qdot/Qdash ensembles and (b) highly inhomogeneous system with broad Gaussian-enveloped DoS/gain profile of Qdot/Qdash ensembles. Adapted from [23] with each ensemble exhibiting a Lorentzian homogeneous broadening profile (c) A schematic describing the spectral coverage by the different quantum-confined active materials on the GaAs- and InP-platforms.

themselves, or both. With that said, with proper optimization of the S-K growth technique, narrow gain profiles are also realizable with nearly uniform Qdots/Qdash dimensions yielding a DoS profile closer to the true/quasi-delta-function ideal case (Fig. 3(a)), hence, resulting in a narrow-band lasing emission if employed as the active region in semiconductor lasers [20].

Fig. 3(c) shows a schematic of the spectral coverage of different quantum-confined nanostructure-based active regions on GaAs- and InP-material platforms. The ~1550 – 1625 nm emission is covered mainly by InGaAsP/InP Qwells and InGaAsP/InP and InGaAlAs/InP Qdots and Qdashes, and are crucial light sources for optical communications. Qwell-based semiconductor lasers are widely applied for short- and long-haul optical fiber communications. InAs/GaAs Qdots was the first choice to realize semiconductor lasers owing to the available mature GaAs material technology, thanks to GaAs – Qwell lasers that propelled this technology in the early 1970s for optical communications. In fact, high-performance narrow-linewidth lasers and the new wave of broadband lasing technology were first demonstrated on InAs/GaAs Qdot lasers in the 1100−1300 nm region. The next logical step was to realize these Qdots on the InP platform for optical communications. However, instead of Qdots, InAs/InP Qdash lasers on the InP platform were realized due to the growth kinetics, as discussed earlier. Since then, significant efforts on optimizing the growth process were in full swing until recently when lasers with InAs Qdots on InGaAlAs- and InGaAsP-InP were successfully demonstrated emitting in the C-band [24].

III. InAs/InP QUANTUM DASH LASER DIODES

Qdash LDs were first introduced in [25] as InAs Qdashes over a substrate of (100) InP as a dash-in-an-asymmetric-well structure that emitted around 1.57 μm and exhibited a slight redshift when more layers of InAs/InGaAlAs were introduced. The laser device was composed of Fabry-Perot (FP) cavity exhibiting several longitudinal modes within the lasing spectrum. The density of the grown Qdashes per layer was estimated to be $\sim 10^{10}$ cm^{-2} with average dimensions of ~5 nm × 25 nm × 300 nm. The reported threshold current density was 410 A/cm^2, while the internal loss and internal quantum efficiency were ~10 cm^{-1} and 60%, respectively. This work encouraged researchers and groups to work on this new class of quantum confined nanostructure-based semiconductor lasers. Not so long afterward, an excellent tunability range was reported in [26] over a FP cavity-based Qdash LD on the same material system whose emission peak ranged from 1.54 to 1.78 μm by changing the thickness of the deposited InAs layers while keeping the threshold current density at the low value of 900 A/cm^2.

As the quality of the growth process improved, better results were reported from Qdash LDs. In [27], the longest reported emission wavelength of 2.03 μm was achieved using a stack of 5 layers of InAs Qdashes embedded in an InGaAs Qwell. In [28], chirping the active region was introduced where different layers of Qdashes were deposited at different stages by varying the barrier layer thicknesses to increase the inhomogeneous broadening of the self-assembled Qdashes and to achieve broad gain materials for semiconductor optical amplifier and broadband laser applications. Different research works have followed the chirped active region technique such as [29] and [30] with FP Qdash LDs exhibiting internal loss values of 4.6 cm^{-1} and 11 cm^{-1}, respectively, and internal quantum efficiencies of 60% and 85%, respectively, while lasing at 1.53 μm and 1.62 μm, respectively. Due to their broadband emission, Qdots and Qdashes are great contenders that can be used in energy-efficient optical telecommunication. The first demonstration of an ultra-broadband Qdash LD was reported in [31] over an InAs/InAlGaAs material system over an InP substrate. The laser emitted at 1.64 μm with a very broad wavelength coverage of 76 nm at room temperature. Later, intermixing (post-growth bandgap engineering) was utilized to widen the coverage to ~85 nm in addition to blue-shifting the emission to the C-band (1.54 μm) with a total emission power of ~1 W [32]. Later, the same group reported 50 nm lasing 3-dB bandwidth at 1.61 μm employing a chirped barrier thickness device active region design [30].

A. QDASH MODE-LOCKED LASERS

A potential application of broadband lasers is in producing extremely short light pulses in the order of picoseconds and femtoseconds, which can be accomplished through mode-locking (ML), where the emitted short pulses are phase-locked depending on the round-trip taken by photons inside the laser cavity. ML can be achieved via an external signal, which is called active ML, or can be achieved passively without an external source, making it more favorable due to its compact nature and lower cost requirements [33]. One of the most straightforward techniques used in passive ML is to divide the device FP cavity length into two sections. The first section is forwardly-biased, acting as the light-emitting laser (amplifier section), while the second section is reversely biased, acting as a saturable absorber that can be used to control and lock the phase of all longitudinal modes [33]. Passive two-sectioned Qdash mode-locked lasers (Qdash MLL) was firstly demonstrated in [34], where a 134-GHz optical pulse train was generated via a 6-layer Qdash MLL with a 940-μm gain and 180-μm absorber sections and an associated beat radio-frequency (RF) linewidth of 47 kHz. Other two-sectioned Qdash MLLs were reported in [35], [36], and [37] with repetition rates of 17 GHz, 10 GHz, and 95 GHz, respectively, with absorber-to-gain section length ratios of 4%, 3.3%, and 10%, respectively.

Since Qdashes possess broad gain profiles and exhibit high absorption rates, the requirements of ML could be easily fulfilled from the same array of Qdashes in a single-section device, where some Qdashes act as absorbers while others contribute to gain. In addition, according to [38], ML in Qdash LDs does not require a saturable absorber but instead

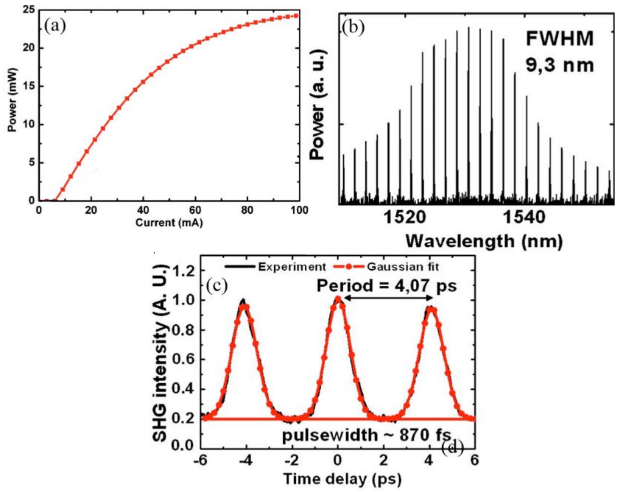

FIGURE 4. (a) L-I characteristics, (b) the lasing emission spectrum, and (c) the autocorrelation trace of the single-sectioned C-band Qdash MLL with a cavity length of 170 μm exhibiting a repetition rate of 245 GHz [39].

utilizes the mutual sideband injection due to four-wave mixing and self-induced carrier density modulation at the free spectral range (FSR) frequency in a similar manner to active ML, albeit by the signal generated from the beating among the laser cavity modes itself instead of an external electrical signal. In turn, this leads to an inherently mode-locked Qdash LD with a single section. This niche characteristic, capable of generating locked equally spaced longitudinal modes with strongly correlated phases, or in other words a comb of equally spaced frequency lines, ultimately resulted in the generation of a periodic signal with a period corresponding to the cavity round-trip time. Moreover, the strong phase-correlation of consecutive modes leads to narrow RF beat tone linewidths. For instance, in [39], sub-picosecond pulse generation was demonstrated over a single-sectioned Qdash MLL with a FP cavity length of 170 μm emitting in the C-band at 1550 nm, as shown in Fig. 4. While Fig. 4(a) shows the measured output light power vs. injected current (L-I) characteristics of the utilized Qdash MLL with a measured threshold current of 6 mA and slope efficiency of 0.52 W/A, Fig. 4(c) shows the autocorrelation trace of the obtained 245 GHz repetition rate. On the other hand, Fig. 4(b) shows the emission spectrum of the Qdash MLL comprised of phase-locked comb lines. Hence, besides finding applications in optical clocks, this new class of Qdash MLL also qualifies as an attractive potential optical frequency comb source in coherent WDM communications and MMW WL 5G and RoF communications. With that said, ML has been observed and well-established in C-band Qdash LDs, and it remains yet to be realized in the L-band region, which has mainly been ascribed to the unoptimized device design and growth process in this wavelength band. Consequently, other techniques, such as optical injection locking and other means of comb generation, have been incorporated as assisting techniques when implementing L-band Qdash LDs in optical communication.

B. QDASH INJECTION-LOCKED LASERS

FP LDs can be forced into a single-mode emission employing assisting optical injection locking (OIL) scheme. When appropriately implemented, the emission of the LD locks into a single emission wavelength mode while suppressing all the side modes, in addition to potentially improving the linewidth, phase noise, relative intensity noise (RIN), coherence, and mode stability significantly [40]. In general, the OIL scheme improves the LD characteristics and relies on optical frequency (wavelength) and phase synchronization techniques. In OIL, the emission of the LD can be locked in terms of frequency and phase to match that of some injected photons into its cavity, thereby improving the mode power of a particular longitudinal mode whose photons matches with the injected photons while suppressing all the other longitudinal modes within the lasing spectrum, thus realizing a single-mode lasing. The injected photons can be generated from a high-quality external master laser, known as external-injection-locking (EIL), or can be acquired employing optical feedback from some of the emitted light of the LD itself, termed as self-injection-locking (SIL) [15]. Although OIL could be applied on any LD, they are of great significance in broadband FP InAs/InP Qdash LDs operating in L-band since the cavity modes within the free-running lasing spectrum suffer from wide linewidths and relatively high phase noise. This is unlike the C-band Qdash MLL discussed in the previous section, where all FP modes exhibit phase-locking with few kHz optical linewidths and reduced phase noise. Unfortunately, inherent single-section ML has not been observed in L-band InAs/InP Qdash laser diodes. Hence, in such a scenario, OIL was deployed to lock the multi-wavelength emission into a single-mode matching the injected light's frequency and phase, all while reducing the phase noise and narrowing the optical linewidth [40]. Moreover, SIL negates the need for a master laser and hence is a cost-effective solution to achieve single-mode lasing emission. Thus, both OIL techniques assist in not only realizing single-mode operation from a Qdash LDs but also reduces the mode linewidth in the frequency domain, *e.g.,* from ~GHz range to ~kHz, besides reducing the noise and increasing the modulation bandwidth [16].

Alternately, OIL is particularly interesting with broadband Qdash LDs as it may be used as a unified colorless source in WDM PONs, where each subscriber at ONU can be assigned a mode (color) out of the same broadband laser device seamlessly by the central office (CO) or OLT via injection locking. In this regard, a large number of FP modes can be obtained from a singular Qdash LD source, allowing for mass deployment of the device as a transceiver since identical devices with identical configurations could be equipped at each OLT/ONU of the WDM-PON, making it much more convenient, and time- and cost-effective when compared to deployment of non-identical sources, thus cutting CapEx and Op-Ex drastically and allows for seamless scalability [13]. Multiple-mode OIL has also been realized to generate a high-quality multi-wavelength Qdash LD in the L-band [41]. In addition, as a

TABLE 1. Summary of the implementation of quantum dash lasers in optical communication in literature in a chronological order.

	Qdash Source	λ [nm]	BW [nm]	#Modes	RIN [dB/Hz]	Modulation Scheme	SMF Length [km]	#Ch.	Data Rate [Gb/s]	Ref.
C-band	MLL	1555	10	8	< -110	OOK	50	8	1×10	[46,47]
	MLL	1550	8	11	< -105	DP-QPSK	BtB	11	1×56	[48,49]
	MLL	1555	12	–	–	OOK	100	4	4×170	[50]
	MLL	1550	7.3	10	< -100	OOK	100	4	4×28	[51]
	MLL	1540	13	43	< -115	16QAM	BtB	37	37×72	[52]
	MLL	1540	13	43	< -115	16QAM	75	13	13×72	[52]
	MLL	1545	13.5	40	< -125	16QAM	3	40	40×28.2	[53]
	MLL	1545	13.5	80	< -125	16QAM	3	80	80×28.2	[53]
	MLL	1550	13.5	16	< -132	16QAM	50	16	16×33.6	[55]
	MLL	1550	13.5	40	< -128	16QAM	50	40	40×33.6	[8]
	MLL	1550	13.5	160	< -125	16QAM	3	160	160×28	[55]
	MLL	1550	12	36	–	DP-QPSK	50	36	36×50	[56]
	MLL	1550	12.5	52	–	DP-QPSK	75	52	52×160	[57]
	MLL	1550	12.5	52	–	16QAM	75	32	32×304	[57]
	MLL	1545	9	50	–	DP-QPSK	75	23	23×180	[59,60]
	MLL	1555	13	48	< -125	PAM4	25	48	48×112	[7,61]
	MLL	1555	13	48	< -130	16QAM	100	48	48×224	[64,65]
	SIL + MLL	1540	12.6	47	–	16QAM	BtB	47	47×256	[66]
	MLL	1555	9	45	< -125	PAM4	1	8	8×56	[67]
	SIL+ MLL	1545	9	55	< -115	32QAM	75	60	60×200	[68,69]
	SIL+MLL	1555	-	8	< -130	OOK	50	5	5×10	[71]
L-band	EIL	1620	10	50 w/ EIL	–	DP-QPSK	10	1	1×100	[70]
	SIL	1605	10	16 w/ SIL	–	DP-QPSK	20	1	1×128	[9,73]
	SIL	1615	10	18 w/ SIL	–	DP-QPSK	10	1	1×168	[74,75]
	EIL	1610	7	14	< -130	QPSK	10	3	3×64	[42,43]

BW: 3-dB bandwidth, RIN: Relative intensity noise for individual filtered modes, #Ch.: Number of channels.

replacement of the unattainable ML in the L-band, OIL has also been engaged to realize an injection-locked Qdash LD comb source based on generating frequency harmonics of the single locked modes which were used in WDM [42], [43] and MMW [44], [45] demonstrations.

IV. QUANTUM DASH LASERS IN FIBER BASED OPTICAL COMMUNICATIONS

Table 1 summarizes the reports in the literature of employing Qdash LDs as sources in different fiber-based single point-to-point and WDM optical communicate systems, operating in the C-band and mid L-band wavelength windows in chronological order. Moreover, the aggregate data rate (*i.e.*, system data capacity) of various fiber-based systems from literature has also been illustrated in Fig. 1(a).

A. C-BAND SMF TRANSMISSION

The first demonstration of implementing a Qdash LD in optical communication was in [46], [47] and illustrated in Fig. 5, where a mode-locked device emitting in the C-band was used to generate a flat comb in the 1550 nm window with 100 GHz-mode spacing. The single-section Qdash MLL was grown via molecular-beam-epitaxy (MBE) over an S-doped (100) InP substrate, with an active region comprised of six layers of InAs Qdashes within InGaAsP Qwell and barrier layers. The Qdash LD was fabricated and cleaved with a cavity length of 420 μm to achieve a mode spacing of 100 GHz in order to match the International Telecommunication Union's (ITU) standard for mode spacing in WDM system. As such, the resulting emission spectrum consisted of a flat-top profile with nearly 12 longitudinal modes available within its 3dB-bandwidth at ~1556 nm, as shown in Fig. 5(a). Regarding the RIN profile, the Qdash MLL exhibited low noise values of < -150 dB/Hz for its total emission power across the measurement range of 20 GHz. This very low RIN profile, compared to Qwell laser diodes counterparts, was attributed to the characteristics of the Qdash material and the low confinement factor associated with the Qdashes (~2.0 %), resulting in a reduced rate of spontaneous emission coupling to the FP modes of the laser diode. On the other hand, the RIN for a single-filtered mode-locked mode was observed to be -110 dB/Hz at low frequencies, which was higher than the entire emission's RIN, and was attributed to the well-known mode-partition noise. The Qdash MLL was incorporated as a source in a WDM system, as shown in the experimental setup of Fig. 5(b), where 8 FP modes were demultiplexed via an array waveguide grating (AWG) demultiplexer (de-MUX) to be separated and utilized as a carrier. The demultiplexed signal showed a side-mode suppression ratio (SMSR) of 35 dB with an optical power of -10 dBm, and then was separately modulated via a $LiNbO_3$ Mach–Zehnder modulator (MZM) in an On-Off Keying (OOK) modulation scheme, *i.e.*, intensity modulation, by a $2^{31} - 1$ long pseudorandom binary sequence (PRBS) at a data rate of 10 Gb/s. The modulated signal was then separately transmitted over a 50 km long

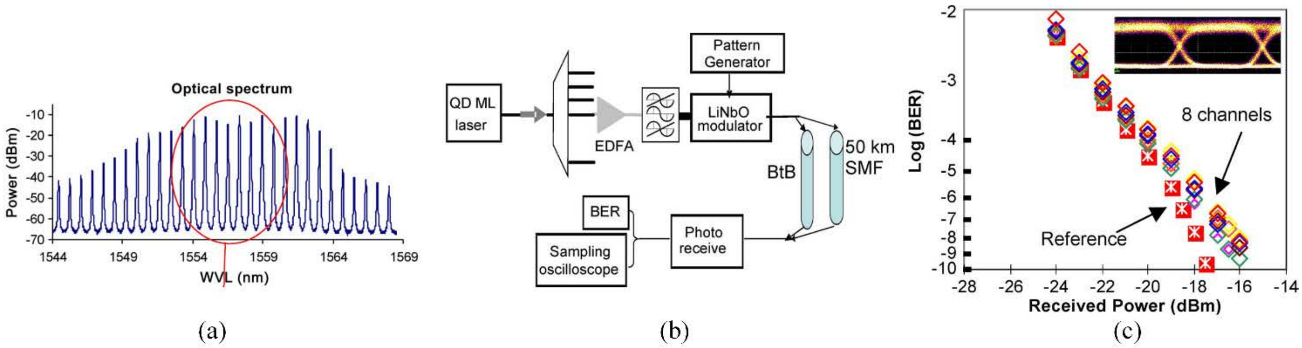

FIGURE 5. (a) Emission spectrum of the C-band Qdash MLL employed in [46], [47]. (b) The utilized experimental transmission setup and the associated (c) BER as a function of the received optical power for each of the eight individually transmitted channels.

SMF in addition to a back-to-back (BtB) configuration for comparison purposes. Fig. 5(c) shows the obtained bit error rate (BER) as a function of the received optical power, verifying successful transmission of this 80 Gb/s capacity system, while its inset shows the eye diagram for one of the received channels.

The following report demonstrated C-band Qdash MLL as a source in phase modulated optical communication system, for the first time [48], [49], which employed a similar Qdash device structure and dimensions to that in [46], [47]. The device showed an emission consisting of 11 modes within its 5dB-bandwidth range of 8 nm at ∼1550 nm with a mode spacing of 100 GHz. In terms of RIN, the device displayed a low value of < -140 dB/Hz across the measurement range of 10 GHz considering all FP modes of the emission spectrum, and < -100 dB/Hz when measured for single filtered mode. The WDM transmission experiment was carried out by employing 11 modes and modulating each mode by a $2^9 - 1$ long PRBS (delayed by 256 bits to decorrelate them) in a dual-polarization quadrature phase-shift keying (DP-QPSK) modulation scheme at a data rate of 56 Gb/s via an MZM. The modulated and multiplexed signal was then coupled into a BtB SMF while an optical filter was used to emulate the de-multiplexing operation at the receiver side by selectively passing each of the modulated carriers to be pre-amplified then demodulated. As such, error-free performance was observed on 9 channels among the 11, and a BER floor of 4×10^{-7} was exhibited by the two extreme modes of the emission spectrum (1550.7 and 1556.5 nm) in addition to displaying a higher power penalty of 5 dB in contrast to 1.5 dB exhibited by the other 9 dominant modes. Both observations were attributed to the higher RIN shown by the extreme non-dominant modes. Nevertheless, this work substantiated the niche features offered by passive single section Qdash MLL that enabled phase locking of all FP modes to emulate an optical frequency comb, hence realizing a 0.5 Tb/s system.

Contemporarily, the same Qdash MLL was also employed in another report but with active ML in the first dense WDM (DWDM)/optical time-division multiplexing (OTDM) transmission utilizing a single Qdash MLL light source [50]. The active ML was achieved via a 42.5 GHz 33% return-to-zero optical clock signal via intensity modulation with MZM. From the emission spectrum of the Qdash LD, 4 modes were extracted by Gaussian filters, creating 4 modes that are 3 nm apart (FSR ∼376 GHz) around 1550 nm. After that, two MZM modulators were used to modulate each of the even and mode channels separately, by a $2^7 - 1$ long PRBS. Then a bit rate multiplier (BRM) multiplexes four delayed versions of the four signals, providing a 4×170 Gb/s DWDM/OTDM transmission (0.68 Tb/s aggregate data rate). Furthermore, the fiber length between each MZM and the BRM was made sufficiently long to decorrelate the odd and even signals. The signals were transmitted through a 100 km long SMF and dispersion-shifted fiber (DSF). Afterward, the received signal was passed through a programmable optical filter to select the desired channel to be detected. This signal pilot an electro-absorption modulator (EAM) that provides optical division demultiplexing and extracts one of the four 42.5 Gb/s tributaries with the aid of an optical delay line. Lastly, the detected signal was pre-amplified and passed through to a standard 42.7 Gb/s electrical time-division demultiplexing receiver for processing and analysis. As such, all four channels were successfully detected with a BER floor of 10^{-8}.

Later, in 2014, an improved WDM transmission was demonstrated in [51], with a single Qdash MLL serving as a transmitter source. However, rather than ∼376 GHz FSR in [50], the mode spacing, in this case, was 100 GHz, matching the ITU WDM standard, thanks to the cleaved cavity length of 420 μm. The emission spectrum of the Qdash MLL constitutes 10 FP modes and exhibited 7.3 nm-3dB-bandwidth at ∼1550 nm. The associated RIN for the entire emission, shown in Fig. 6(a), measured < -135 dB/Hz across the 10 GHz measurement span and < -100 dB/Hz for filtered out single modes. In terms of the transmission experimental setup, shown in Fig. 6(b), the Qdash MLL's emission was amplified by an Erbium-doped fiber amplifier (EDFA), which was then passed through a multiport filter, to extract four modes as channels for transmission, each was followed by a semiconductor optical amplifier (SOA) to reduce the RIN of each filtered mode further. The transmission experiment was carried out with and without said SOAs. Nonetheless, the 4 FP modes were then combined by optical couplers into two paths; even and odd modes, where

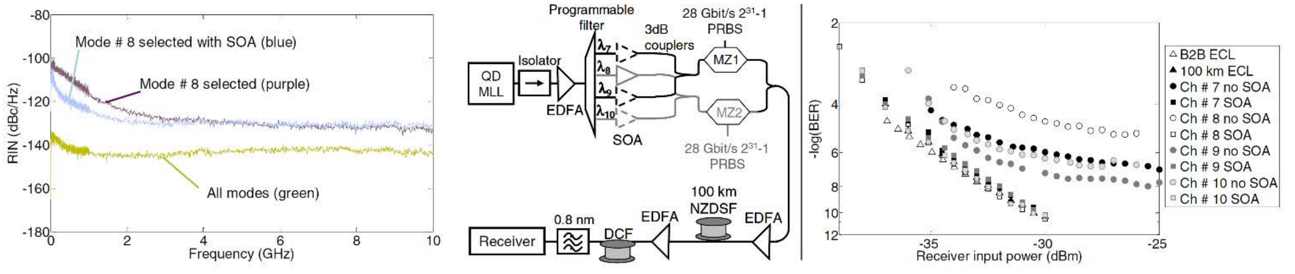

(a) (b) (c)

FIGURE 6. (a) RIN profile of the C-band Qdash MLL implemented in [51] for the entire emission spectrum and for sampled filtered mode with and without the SOA (b) WDM transmission experimental setup demonstrated in [51]. (c) The associated BER as a function of received optical power with and without the SOAs at the transmitter side.

each was modulated in the OOK scheme by a separate MZM driven by a $2^{31} - 1$ long PRBS at a data rate of 28 Gb/s (112 Gb/s aggregate data rate). Then, the even and odd paths are combined via another optical coupler, and the combined multiplexed signal was amplified and transmitted over a 100 km long non-zero dispersion-shifted SMF with a chromatic dispersion of +5 ps/nm.km at 1550 nm. At the receiver side, the signal was amplified and passed through the dispersion compensation fiber (DCF), and the desired channel was subsequently extracted via a 100 GHz optical filter to be detected. Fig. 6(c) depicts the BER as a function of the received optical power for all four channels, with and without the SOAs. The observed BERs showed successful transmission with error floors between 10^{-5} and 10^{-8}. Moreover, deployment of SOA drastically improved the BER across the 4 channels showing <0.5 dB penalty and a BER floor of 10^{-9}, identical to the performance of a commercial external cavity laser (ECL) employed as a reference case. In other words, the RIN reduction resulting from the SOA, evident in Fig. 6(a), led to penalty removal and error floor suppression.

One year after, two reports, *viz.* [52], [53] simultaneously demonstrated the first Tb/s data-capacity WDM transmission with a single Qdash MLL source, and both incorporating 16-quadrature amplitude modulation (16QAM) as a modulation scheme. This was challenging to implement with a free-running Qdash LD due to inherently broad optical linewidths of the FP modes in the order of tens to hundreds of MHz [54]. However, engaging Qdash MLL, the locked comb lines exhibited significantly reduced linewidths, thanks to phase-locking of all modes. Reference [52] realized a 16QAM transmission by implementing self-homodyne coherent detection and splitting the emission of the Qdash MLL into two halves: one to be modulated and transmitted alongside the other unmodulated half to act as a local oscillator (LO). The Qdash MLL emission spectrum consists of 43 comb lines centered at ∼1540 nm with a mode spacing of 42 GHz (*i.e.*, 980 μm cavity length) and RIN values < −115 dB/Hz for sampled filtered out single modes. The emission was split into the two halves via an optical coupler where the first half is dis-interleaved into even and odd modes where each was modulated independently with a $2^{11} - 1$ long PRBS in a 16QAM scheme at a symbol rate of 18 Gbaud (72 Gb/s). After that, the even and odd comb lines were merged via an optical coupler before the data stream was recombined with the unmodulated comb lines on orthogonal polarization via a polarization beam combiner (PBC). The signal was then transmitted over BtB and 75 km long SMF. A polarization controller and a PBS were utilized at the receiver side to separate the modulated comb lines from the unmodulated LO comb lines. Finally, in order to detect and demodulate the desired channel, two optical filters were identically tuned to extract the desired channel and its corresponding LO. An optical modulation analyzer (OMA) was utilized to perform self-homodyne coherent detection to analyze the recovered signals. In addition, optical tunable delay lines were used to match the group delay for both the modulated and LO signals to reduce the phase noise effects. In the BtB transmission experiment, out of the transmitted 43 comb lines, 37 (41) channels exhibited BER values below the forward error correction (FEC) limit with an overhead of 7% (20%), corresponding to a post-FEC net aggregate data rate of 2.678 Tb/s. On the other hand, in the 75 km long SMF transmission experiment, only 13 (25) channels displayed BER values below the FEC limit with an overhead of 7% (20%), corresponding to a post-FEC net aggregate data rate of 1.567 Tb/s.

Concurrently, in reference [53], Vujicic *et al.* employed a passive Qdash MLL grown by MBE on an S-doped (001) InP substrate with an active region comprised of 9 layers of InAs Qdashes separated by InGaAsP barrier layers. The device was fabricated as buried-ridge stripe waveguide lasers and was cleaved at cavity lengths of 950 and 1870 μm, corresponding to a FSR of 44.7 GHz and 22.7 GHz, respectively. In addition, the shorter and longer cavity length devices exhibited a 3-dB bandwidth of 13 nm with 40 and 80 modes, respectively, with measured mode optical linewidth in the range of 10-20 MHz. Both devices displayed a low value of < −140 dB/Hz for the entire spectrum across the 10 GHz measurement range in terms of the RIN. However, the measured RIN for individual modes ranged between −125(−122) and −132(−129) dB/Hz for the 44.7(22.7) GHz Qdash MLL. Both devices were incorporated as sources in the WDM transmission experiment setup shown in Fig. 7(a) [53]. An EDFA amplifies the Qdash

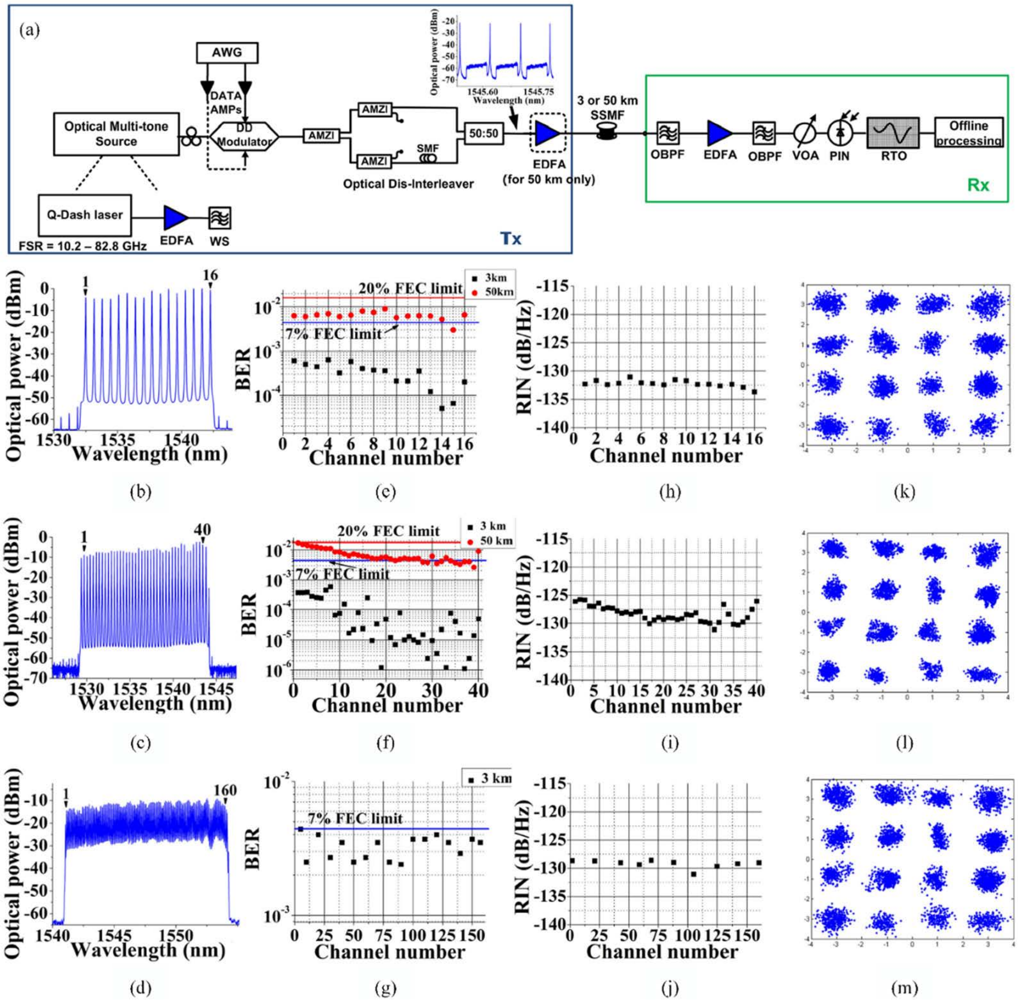

FIGURE 7. (a) WDM transmission experimental setup demonstrated in [53] and [55] employing C-band Qdash MLL. The emission spectrum of the (b) 82.8, (c) 44.7, and (d) 10.2 GHz Qdash MLLs. The measured BER of each comb line of the (e) 82.8, (f) 44.7, and (g) 10.2 GHz Qdash MLLs. The measured RIN of each comb line of the (h) 82.8, (i) 44.7, and (j) 10.2 GHz Qdash MLLs after detection and processing. Constellation diagram of the modulated middle channel of the (k) 82.8, (l) 44.7, and (m) 10.2 GHz Qdash MLLs after transmission through the 3 km SMF.

MLL emission spectrum, and then a waveshaper is employed to select the desired number of channels. Thereafter, the filtered comb lines were modulated by a dual-drive MZM at a data rate of 28.2 Gb/s in a 16QAM modulation scheme. Next, tunable cascaded dis-interleavers based on an asymmetric Mach Zehnder interferometers (AMZI) were utilized to split the modulated comb into even and odd parts, which were then decorrelated, recombined, and transmitted through a 3 km long SMF. The desired channel was filtered with an optical band-pass filter (OBPF) at the receiver side before amplifying with an EDFA. The filtered channel was then detected by a 10 GHz receiver consisting of a *pin* photodetector and an integrated trans-impedance amplifier (TIA) and then captured with a real-time oscilloscope (RTO) operating at 50 GSa/s. As such, all 40 modes of the 44.7 GHz Qdash MLL exhibited a BER $<$ 7% FEC threshold, indicating an aggregate capacity of 1.128 Tb/s (40 $\times$ 28.2 Gb/s). On the other hand, the 22.7 GHz Qdash MLL counterpart exhibited 77 (80) modes with a BER $<$ 7% (20%) FEC limit, corresponding to a data capacity of 2.256 Tb/s.

Right afterward, Vujicic *et al.* extended their work by implementing C-band Qdash MLLs in different WDM SMF configurations [55]. In particular, three Qdash MLL diodes of cavity lengths of 550, 950, and 4000 μm, and sharing the same active region's structure employed in reference [53]. The resulting FSRs were 82.8, 44.7, and 10.2 GHz, respectively, with 16, 40, and 160 comb lines within their respective bandwidths at $\sim$1540 nm, as depicted in Figs. 7(b)−(d) [55]. Regarding RIN, 82.8, 44.7, and 10.2 GHz Qdash MLLs exhibited < -144, < -143, and < -133 dB/Hz, respectively, for the entire emission spectrum. On the other hand, the RIN of filtered individual modes ranged from -131 to -134 dB/Hz, -125 to -132 dB/Hz, and -125 to -132 dB/Hz, for the 82.8, 44.7, and 10.2 GHz Qdash MLLs, respectively, as depicted in Figs. 7(h)−(j). The transmission setup was identical to [53] and is shown in Fig. 7(a).

Each of the three Qdash MLLs was incorporated as a single source in the WDM transmission system. Firstly, each comb was dis-interleaved into even and odd, then modulated in a 16QAM scheme at a data rate of 28.2 Gb/s and recombined and transmitted through a 3 km long SMF in a similar manner. Figs. 7(e)−(g) show the measured BER for the 82.8, 44.7, and 10.2 GHz Qdash MLLs, respectively, showing successful transmission of all modes with BER $<$ 7% FEC threshold with an aggregate data rate of 451.2 (16 $\times$ 28.2 Gb/s), 1.128 Tb/s (40 $\times$ 28.2 Gb/s), and 4.5 Tb/s (160 $\times$ 28.2 Gb/s), respectively [55]. Figs. 7(k)−(m) show the received 16QAM constellations of the modulated central channel of the 82.8, 44.7, and 10.2 GHz Qdash MLLs, respectively. Next, the 82.8 and 44.7 GHz devices were investigated over a 50 km long SMF WDM transmission experiment by replacing the 3km long SMF. Figs.7 (e) and (f) show the obtained BER for both devices, respectively, with BER values below the 20% FEC limit for all respective modes after transmission over the 50 km long SMF. Besides, a similar experiment was also reported in reference [56] with 33.4 GHz FSR Qdash MLL of cavity length 1250 μm. In this work, 36 comb lines were transmitted similarly through 50 km SMF, demonstrating a net aggregate data rate of 1.8 Tb/s (36 $\times$ 50 Gb/s) with a DP-QPSK modulation scheme.

The subsequent report demonstrated a maximum spectral efficiency system in C-band [57] where a Qdash MLL with a similar active region configuration in [46], [47] and cavity length of 980 μm, corresponding to an FSR of 42 GHz, was employed. The lasing emission spectrum exhibited a 3-dB bandwidth of $\sim$12.5 nm, comprising 50 FP modes at $\sim$1550 nm. The measured optical linewidths were in the range of 7 – 12 MHz. This broadened optical linewidth was attributed to several effects such as coupling spontaneous emission into the oscillating mode leading to spectrally white frequency noise, flicker, and random-walk frequency noise. Thus, this work introduced a digital symbol-wise blind phase search (BPS) technique to improve coherent detection, thereby avoiding any hardware-based phase-noise compensation. The transmission experiment was implemented with a single Qdash MLL source, where 52 comb lines were split into odd and even halves through a programmable optical filter. The even and odd carriers were amplified, and then each half was modulated by a $2^{11} - 1$ long PRBS in DP-QPSK modulation scheme at a symbol rate of 40 Gbaud (160 Gb/s). The data stream was later transmitted through a 75 km long SMF. At the receiver side, optical filters were used to select the desired channel, then amplified and detected on a dual-polarization coherent receiver whose output was digitized and recorded for offline digital signal processing, mainly chromatic-dispersion compensation and BPS to eliminate the drastic effects of phase noise. The BER of all 52 channels was observed to fall below the 7% FEC threshold, which ultimately indicated the successful transmission with an aggregate data rate of 8.32 Tb/s transmitted over a 75 km long SMF with a net spectral efficiency of 3.8 bit/s/Hz [58]. Furthermore, the transmission experiment was repeated with 38 comb lines with a DP-16QAM modulation scheme at a symbol rate of 38 Gbaud (304 Gb/s) with the aid of symbol-wise BPS to demonstrate its viability. Indeed, it was shown that out of the 38 channels, 32 fell below the 7% FEC threshold BER while all 38 fell below the 20% FEC limit, leading to a net data rate of 10.68 Tb/s with a net spectral efficiency of 6.7 bit/s/Hz.

Concurrently, the same team demonstrated another WDM transmission experiment in references [59], [60] by employing two Qdash MLLs for the first time; one as a comb source at the transmitter side and another as a comb LO at the receiver side. In coherent detection, it is paramount to maintain a low frequency and phase offset between the carrier of each channel and the corresponding LO tone at the receiver. The buried ridge waveguide Qdash MLLs device structure was similar to reference [57] with a cavity length of 1.71 mm, leading to an FSR of 25 GHz with overlapping spectra at appropriately set injection currents and temperature points, as depicted in Fig. 8(a), taken from reference [59]. The FSR difference (ΔFSR) between both combs was measured to be 4 MHz at a current injection of 278 mA and 125 mA for the transmitter (Tx) Qdash MLL comb LO Qdash MLL comb, respectively. The 3-dB bandwidth of the LO comb demonstrated a smaller value than the Tx comb, as shown in Fig. 8(a), thereby limiting the number of WDM channels of the system. This was ascribed to the higher operating temperature of the LO comb due to its high thermal resistance. Then, the optical linewidth of the transmitter carrier and the receiver LO was obtained by beating matching single modes from each device on balanced photodetectors. As such, the beat note between both devices showed a 5.1 MHz linewidth. Such a broad beat tone linewidth inhibited using higher-order modulation formats, and instead, the DP-QPSK modulation scheme was adopted alongside the symbol-wise BPS algorithm. The experimental setup is depicted in Fig. 8(b). The Tx Qdash MLL emission spectrum comprised 23 spectral lines in C-band at $\sim$1545 nm, which are amplified and dis-interleaved into odd and even halves via a programmable filter. The filter was set to pass every second comb line of the 25 GHz Tx Qdash MLL to achieve 50 GHz spacing to satisfy the ITU standard for DWDM, in addition to flattening the comb spectrum. Then, each half was modulated independently by a $2^{11} - 1$ long PRBS in DP-QPSK modulation format at a symbol rate of 45 Gbaud, which corresponds to 180 Gb/s per carrier. The modulated even and odd carriers were then recombined by a polarization-maintaining 3-dB coupler to form a DWDM stream with uncorrelated data streams on adjacent channels. The upper plot of Fig. 8(c) shows the overlapped emission spectra for both the even and odd combs before modulation, measured at point P1 of Fig. 8(b). The dual-polarization is achieved by polarization division multiplexing (PDM) consisting of a polarization-maintaining 3-dB coupler, $\sim$5.34 ns (240 symbols) optical delay line, and PBC. The multiplexed signal was amplified and transmitted over a 75 km long SMF. At the receiver, the DWDM channel of interest was selected via a 0.6-nm

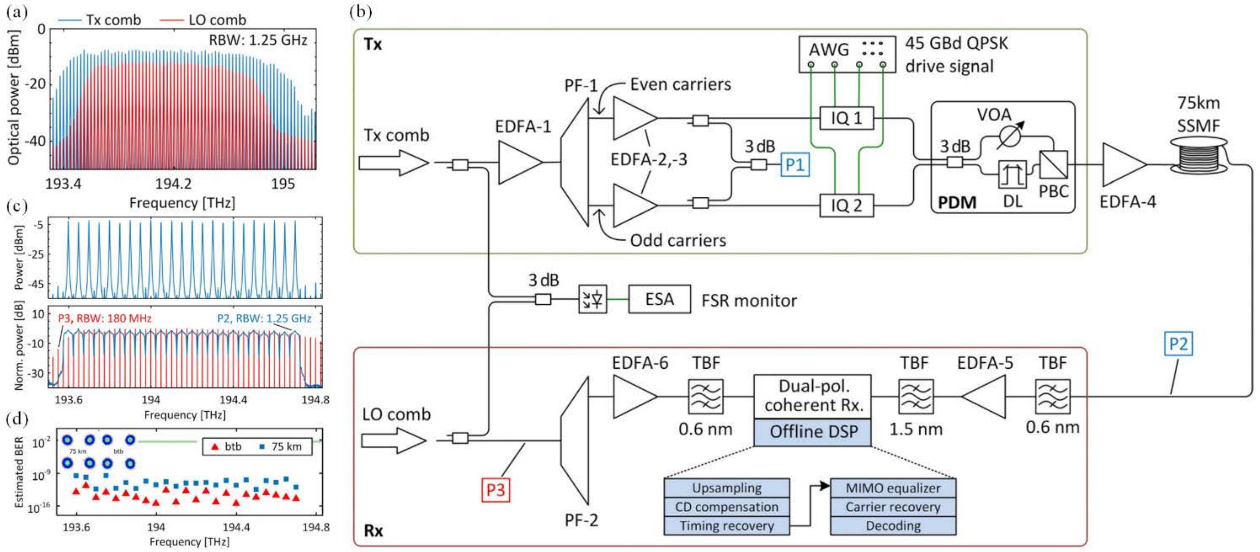

FIGURE 8. **(a) Emission spectrum of the C-band Tx and LO Qdash MLL employed in [59]. (b) The utilized experimental transmission setup. (c) Comb spectra of both even and odd carriers before modulation (upper plot, P1), the spectrum of 23 modulated carriers (lower plot, P2), and the spectrum of the LO comb (lower plot, P3). (d) BER of the 25 comb lines after transmission through the BtB and 75-km SMF. The inset of (d) shows an example constellation diagram for a sample comb line at 194.15 THz.**

tunable band-pass filter, boosted by an EDFA, and filtered again to suppress the out-of-band amplified spontaneous emission (ASE) noise of the EDFA. The chosen channel was detected by a dual-polarization coherent receiver, while the corresponding reference tone for coherent detection was selectively passed from the LO Qdash MLL comb using a programmable filter and then amplified and filtered. The output of the coherent receiver was digitized using four oscilloscope channels with a sampling rate of 80 GSa/s each and evaluated offline using digital signal processing, particularly carrier phase noise compensation based on BPS. The lower plot of Fig. 8(c) shows the spectra of the 23 modulated carriers after transmission (measured at point P2 in Fig. 8(b)) and of the LO comb (measured at point P3 in Fig. 8(b)). The transmission results are plotted in Fig. 8(d), where 23 detected comb lines, after transmission through the BtB and 75 km long SMF, fell below BER of 10^{-9}, far less than the 7% FEC threshold indicating successful transmission of all channels with net aggregate data rate 3.87 Tb/s. The inset of Fig. 8(d) shows an example constellation diagram for a sample comb line after transmission through both links.

Four-level pulse amplitude modulation (PAM4) was first incorporated as a modulation scheme in the Qdash MLL based WDM communication system [7], [61]. PAM4 has been obtaining substantial attention due to its simplicity and reliable performance compared to other high-order modulation schemes such as 16QAM [55], [62], [63]. The employed Qdash MLL device structure was grown by chemical beam epitaxy on exactly (001) oriented n-type InP substrates with 5 stacks of InAs Qdashes within InGaAsP barrier layers. The device was fabricated as a ridge-waveguide FP laser diode with a ridge width of 2 μm and a cavity length of 1227 μm, resulting in an FSR of 34.2 GHz. The lasing emission of the Qdash MLL was centered at 1554.22 nm with a 6-dB bandwidth of 13 nm, including 48 modes. The RIN of individual filtered modes was in the range -125 to -130 dB/Hz over the measurement range of 10 GHz with an average of -128 dB/Hz, while the RIN of the entire emission was < –140 dB/Hz. In terms of the optical linewidth, the average of each mode was measured using the delayed self-heterodyne technique as $\sim$1.55 MHz, and being broader at the fringes with exhibited 3 MHz value. Besides, single-sideband frequency noise was also measured to be < 10^{10}Hz^2/Hz over a range of 100 Hz to 1 MHz, indicating a strongly suppressed phase noise and attributed to the low ASE noise and low confinement factor Qdashes. Next, the WDM transmission experiment was performed by filtering out individual mode-locked FP modes via an optical filter to be modulated by $2^{15}-1$ long PRBS in PAM4 format at a symbol rate of 28 Gbaud via a MZM and PDM (112 Gb/s per channel). The modulated signal was then amplified and transmitted through a 25 km long SMF to be amplified again at the receiver, where an OMA was used to coherently detect the signal using a LO matching the modulated signal. The BER results are shown in Fig. 9(a) for two such modes, and the received eye diagram for the BtB and SMF transmission in Fig. 9(b) [7], [61]. As such, successful communication was achieved for all the 48 individually transmitted comb lines with BER below the FEC threshold, while some achieved error-free operation (BER < 10^9), with a BER floor around -15 dBm. This work was expanded later in references [64] and [65] by implementing PDM 16QAM at 28 Gbaud (224 Gb/s) over 48 transmitted modes in addition to extending

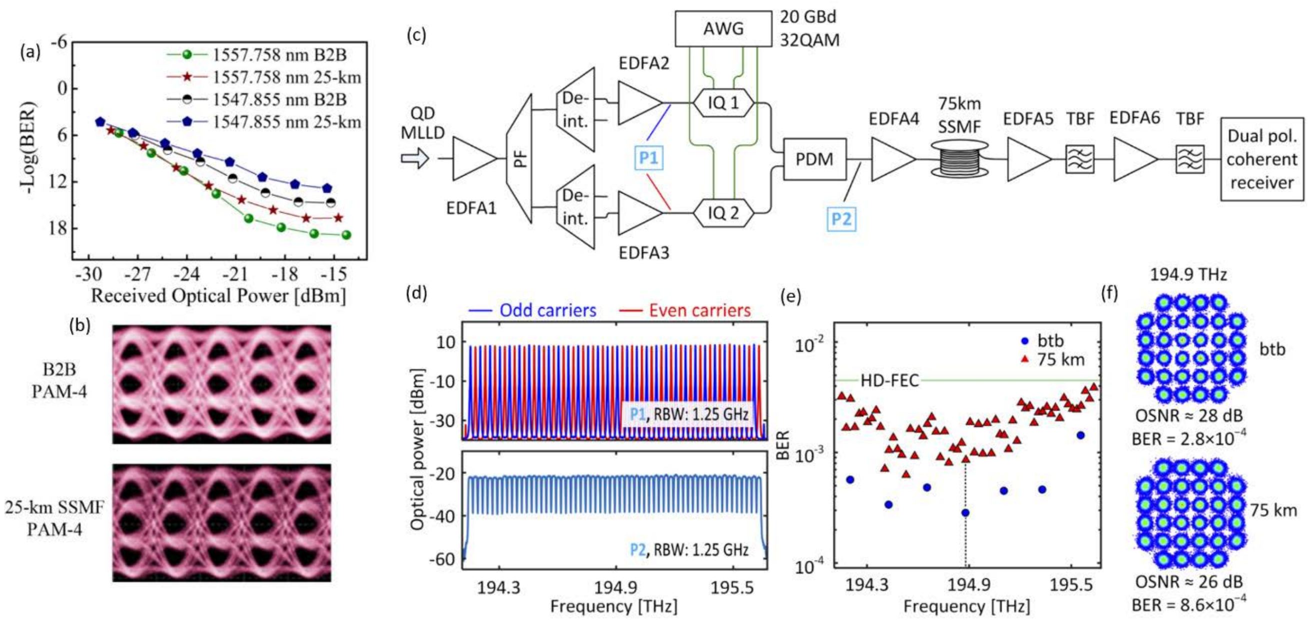

FIGURE 9. (a) The experimental transmission setup demonstrated in [68, 69] employing C-band Qdash MLL. (b) Combined spectra of both unmodulated odd and even carriers taken at position P1 (top) and spectrum of the 60 modulated comb lines measured at position P2 (bottom). (c) BER of the different transmitted channels in BtB and 75 km long SMF links. (d) Example constellation diagrams of the mode at 194.9 THz. BER versus the received power for the BtB and 25 km SMF for PAM-4 transmission across various comb lines of C-band Qdash MLL [7], [61].

to SMF length from 25 to 100 km, exhibiting an aggregate data capacity of 10.8 Tb/s.

Later, in reference [66], the achieved aggregate data rate was pushed further by applying SIL over the same Qdash MLL to reduce the optical linewidth further. This was accomplished by coupling laser light from the read-facet into a lensed polarization-maintaining fiber and then constructing a feedback loop back into the laser via an optical circulator and a variable optical attenuator. It was shown that any single mode in the range of 1531.60 nm to 1544.20 nm could be locked, with demonstrated reduction in the optical linewidth from 0.9 MHz to <300 kHz. This enabled the 47 comb lines of the SIL Qdash MLL to be modulated with 16QAM at 32 Gbaud (256 Gb/s) while employing PDM and transmitted over a BtB link. Error-free transmission of all the modes was achieved, leading to an aggregate data rate of 12 Tb/s.

Another PAM4 implementation was reported soon after in [67] with a C-band Qdash MLL whose gain medium consisted of 3 layers of InAs Qdashes with an FSR of 32.5 GHz. The emission spectrum constituted 45 FP modes within its 3-dB bandwidth of 9 nm (194.979 to 195.204 THz), whereas the RIN of an individually filtered showed < -135 dB/Hz. In the WDM transmission experiment, a wavelength selective switch (WSS) was used to pass 8 comb lines out of the emission of the Qdash MLL with the aid of a tunable delay line interferometer (DLI) to filter and decorrelate the odd and even 32.5 GHz-spaced WDM channels. Then the comb lines were modulated via a MZM at a data rate of 56 Gb/s and transmitted through a 1 km long SMF. The desired channel is filtered, amplified, detected, and captured on a RTO at the receiver side. All 8 channels showed BER below the 20% FEC limit, with channel number 5 (8) performing the worst (best) with a BER of $1.2 \times 10^{-3} (2.5 \times 10^{-3})$, thus indicating successful aggregate 448 Gb/s transmission over a 1.3 THz-frequency range, yielding a spectral efficiency of 1.54 b/s/Hz.

Further performance improvement of Qdash MLL used in [59] with 1710 μm length was shown in references [68], [69]. In this work, with the aid of external-cavity feedback, as a form of SIL, the phase noise characteristic of the source was enhanced, thus improving the optical linewidth and the transmission performance. This new broadband laser device reported the first 32QAM modulation scheme transmission over a single C-band Qdash MLL, leading to the best spectral efficiency. The external cavity was formed by the cleaved facet of the Qdash MLL and a highly reflecting plane metallic mirror, placed 30 cm away from the facet. A plano-convex lens collimated the beam emitted from the laser, while a variable attenuator was used to adjust the cavity's quality factor, thereby adapting the level of optical feedback to avoid unstable operation. The mirror position was manually adjusted such that the cavity length was close to an integer multiple of the effective optical length of the FP laser cavity. In particular, the device FSR was set 50 times the external cavity's FSR. In this configuration, the simultaneous feedback for all lines qualitatively preserves the flat and broadband spectral envelope of the Qdash MLL, unlike the case of single- or dual-mode injection locking. The SIL

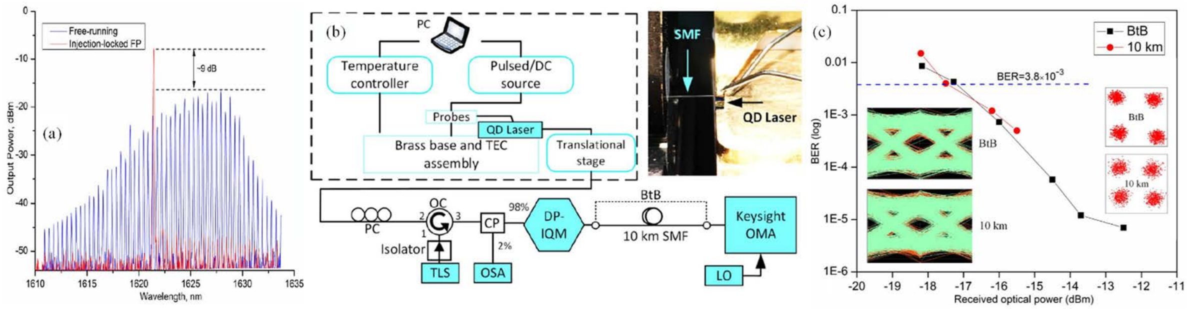

FIGURE 10. (a) The emission spectrum of the mid L-band Qdash LD, reported in [71], before and after injection locking. (b) The implemented experimental transmission setup. (c) The BER of the received modulated signal as a function of the received optical power. The insets show the constellation and eye diagrams for the BtB and 10-km SMF channels.

emission spectrum of the Qdash MLL included 50 FP modes within a 3-dB bandwidth of 9 nm centered at 1545 nm with an optical signal-to-noise ratio (OSNR) of >36 dB. Without the external-cavity feedback, the optical linewidth of the modes was measured to be 1.1 MHz. However, after implementing the external-cavity feedback SIL configuration, the optical linewidth drastically reduced to 34 kHz, corresponding to a reduction of approximately two orders of magnitude, which was similarly observed in the frequency noise profile as well. The RIN was < -115 dB/Hz for single filtered modes without any substantial improvement with external-cavity feedback. After that, the feedback-stabilized Qdash MLL was implemented as a source in a WDM transmission experiment, shown in Fig. 9(c) [68], [69], wherein odd and even modes were split via a programmable filter and a dis-interleaver. Then the signal was amplified and modulated in a 32QAM modulation scheme at a symbol rate of 20 Gbaud by a $2^{11}-1$ long PRBS and engaging PDM (200 Gb/s per channel). Fig. 9(d) shows the combined spectra of both unmodulated odd and even carriers taken at position P1 (top spectrum) and of the 60 modulated comb lines measured at position P2 (bottom spectrum). Then, after amplification, the recombined and modulated comb lines were transmitted over a 75-km long SMF in addition to a BtB link. The desired comb signal was filtered out at the receiver, amplified, and detected on an OMA. As shown in Figs. 9(e) and (f), the BER for all 60 comb lines was found to fall below the 7% FEC limit yielding a record net data rate of 11.215 Tb/s with a net spectral efficiency of 7.5 b/s/Hz.

Lastly, a SIL scheme, used in reference [9], was employed on the C-band 1555 nm Qdash MLL in [70], wherein 8 locked modes from the 840 μm cavity length laser device were used. More details about the SIL technique have been discussed in the subsequent section. This assured 50 GHz FSR of Qdash LD, thus satisfying the ITU grid requirements. The device comprised of 6 layers of InAs Qdashes separated by InGaAsP barrier layers on InP and fabricated into buried ridge waveguide FP laser devices. 5 modes were then externally modulated with 10 Gb/s baseband amplitude shift keying (ASK) singnal, or OOK, and transmitted over 50 km SMF before 4 modes being converted into MMW 100 GHz (λ_1, and λ_3) and 50 GHz MMW (λ_7 and λ_8) signals for further downlink transmission. In contrast, one optical mode λ_5 was used for the baseband downlink signal successfully received by a 10 GHz photodiode and BER tester. More details about the MMW downlink transmission have been discussed in section VI-A.

B. L-BAND SMF TRANSMISSION

As stated earlier, Qdash LDs stand out as potential candidates with demonstrated emission in a wide range of wavelengths covering the S- to U-bands. In particular, L-band Qdash LDs are of interest from the outlook of future NG-PONs, whose primary goals are to maximize the per-user capacity, increase the number of subscribers and extend the network range [3], [4]. Hence, unrestricting the utilizable bandwidth from a well-exhausted C-band and extending to the L-band region would be a natural evolution [1]. Thus, realizing a multi-wavelength source in the L-band region, mainly mid and far L-band region (i.e., >1608 nm), has further strengthened the potential of InAs/InP Qdash LDs as strong contenders for source-unified NG-PON paradigms. However, investigating L-band Qdash LDs as a source in transmission experiments is challenging since the device epitaxy growth process has not been fully optimized, unlike the previously reported high-quality C-band Qdash LDs. Moreover, the limitation of the wavelength-incompatibility with the commercially standardized and optimized C-band optical communication equipment and hardware renders the L-band Qdash LD investigation more demanding.

Nevertheless, the first point-to-point transmission experiment employing L-band Qdash LD was demonstrated in [71] with the aid of EIL at ~1625 nm. The device structure was grown by MBE over a (100) oriented S-doped n-type InP substrate. The active region was chirped by varying the thickness of the barrier layers atop each of the four InAs Qdash stacks, which was done intentionally to increase the active region inhomogeneity further and achieve a broader gain profile [72]. The device was fabricated as a ridge-waveguide FP laser diode with a cavity length of 800 μm and a ridge width of 4 μm. The free-running emission of the Qdash LD, depicted in Fig. 10(a) with a 3-dB bandwidth of 10 nm

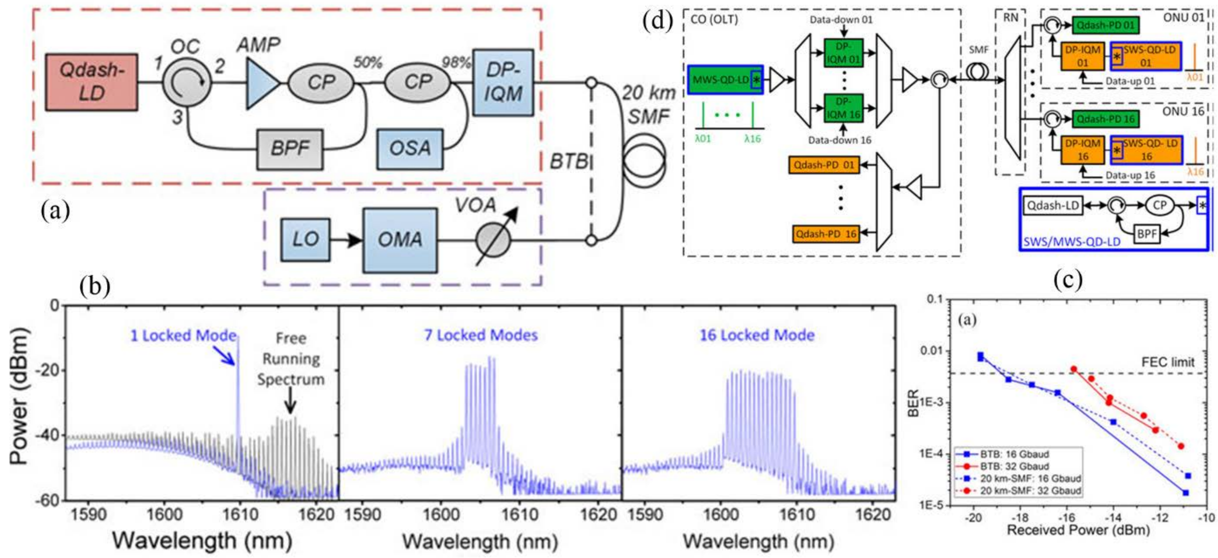

FIGURE 11. (a) The implemented experimental transmission setup incorporating mid L-band SIL Qdash LD [9, 73]. (b) SIL of the Qdash LD showing a single locked mode along with the free-running spectrum, 7, and 16 locked modes. (c) The BER of the received modulated self-injection locked mode as a function of the received optical power. (d) Proposed WDM-PON architecture based on self-seeded Qdash LDs as a multi-wavelength source. MWS-QD-LD: Multi-wavelength Qdash LD, SWS-QD-LD: Tunable Single wavelength Qdash LD.

and FSR of 40 GHz [71]. However, due to broad optical linewidths exhibited by the longitudinal modes, optical feedback, in the form of EIL, was employed to frequency stabilize the operation of the Qdash LD by reducing its noise characteristics, and hence, optical linewidth. The experimental setup of EIL and optical transmission is illustrated in Fig. 10(b), where the light of a single-mode commercial tunable laser source was injected into the Qdash LD cavity with the aid of an optical circulator. When matched to one of the Qdash LD's modes, the injected light locks that particular FP mode while suppressing the other modes to enable employing as a carrier for coherent communication. Fig. 10(a) also shows external the injection-locked emission of the bare (unmounted and unbonded) Qdash LD when locked to 1621 nm with a side-mode-suppression-ratio (SMSR) of 38 dB. The locked mode tuning range was 23 nm, from 1611 nm to 1634 nm, thus encompassing 50 FP modes to which the Qdash LD can be injection-locked and potentially serve as subcarriers in WDM systems. The optical transmission was performed by modulating the 1621 nm locked mode by a $2^{11} - 1$ long PRBS in DP-QPSK modulation scheme at a symbol rate of 25 Gbaud (100 Gb/s). The modulated signal was then transmitted over a 10 km SMF, received, and processed on an OMA without employing any EDFA in the system. A successful transmission with BER below the FEC threshold of 3.8×10^{-3} is depicted in Fig. 10(c), with insets showing the constellation and eye diagrams for the BtB and 10-km SMF channels at a received power of -15.5 dBm.

Soon after, EIL was replaced with the SIL paradigm in the mid L-band optical communication [9], [73]. In this work, a Qdash LD based on the same active region with a cavity length of 600 μm and a ridge width of 3 μm, emitting at ~1610 nm with a 3-dB bandwidth of 8-10 nm was utilized. Compared to EIL, SIL poses a more attractive solution to stabilizing the performance of the laser as it negates the need for an external active seeding source and the associated cost and power requirement of the system. SIL was accomplished by selectively injecting the desired FP modes out of the free-running emission of Qdash LD in a feedback loop consisting of EDFA, OBPF, and optical circulators, as illustrated in Fig. 11(a) [9], [73]. In this configuration, any or all 16 FP modes within the 1600-1610 nm window could be selectively locked, as shown in Fig. 11(b), by tuning the OBPF. The SMSR of the locked modes ranged from 38 to 22 dB. In addition, only half of the Qdash LD's emission between 1600 to 1610 nm was utilized due to the bandwidth limitation of the EDFA. Nonetheless, a single FP mode at 1609.6 nm was SIL and deployed as a subcarrier in the optical communication experiment, illustrated in Fig. 11(a). The mode was modulated by a PRBS of length $2^{11} - 1$ with DP-QPSK format at symbol rates of 16 Gbaud (64 Gb/s) and 32 Gbaud (128 Gb/s). The modulated signal was then transmitted through a 20 km SMF and BtB configuration. An OMA served as the receiver for detection and processing with the aid of an external LO. Fig. 11(c) shows the obtained BER as a function of the received power where both data rates exhibited BERs below the FEC limit over the 20 km SMF transmission. Later, the same SIL Qdash LD was utilized in another demonstration [74], [75] in which the symbol rate was increased to 168 Gb/s over a transmission link of 10 km-SMF.

As pointed out earlier, ML has not yet been realized in L-band Qdash laser diodes. However, their broadband emissions could be exploited with OIL assisting technique

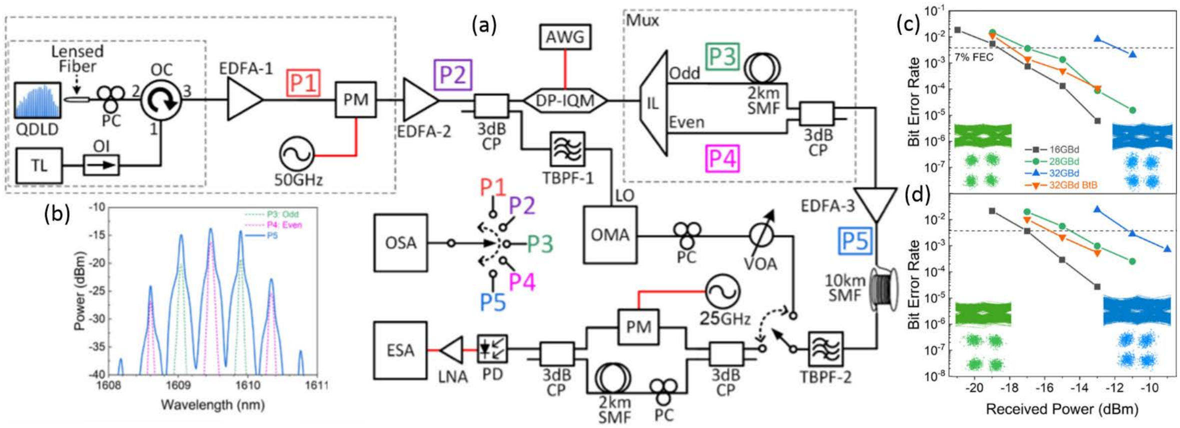

FIGURE 12. (a) The implemented experimental DWDM transmission setup employing the EIL Qdash LD based comb source [42], [43]. (b) The unmodulated odd and even modes of Qdash LD based comb source lines at locations P3 and P4 alongside the recombined 32-Gbaud modulated comb source at location P5. The transmission performance of the two received carriers, (c) left and (d) central modes at different data rates, and insets depicting the QPSK constellation and eye diagrams.

for potential deployment as a unified optical transceiver in NG-PONs. With this viewpoint, a WDM-PON architecture based on SIL Qdash-LD as a multi-wavelength source at CO and broadly tunable single wavelength source at ONUs was also proposed in [9] and illustrated in Fig. 11(d). The architecture could exhibit a potential data capacity of 2 Tb/s (16 × 128 Gb/s) in mid L-band. Furthermore, it was also argued that the SIL loop could be replaced by a customized tunable fiber Bragg gratings (FBG) to simplify the proposed transmitter design.

Lastly, this section is concluded by the recent first demonstration of the simultaneous transmission of multi-carriers in the mid L-band in a DWDM configuration using a single Qdash LD, reported in [42], [43]. The device employed was 700 μm-cavity length and 4 μm-ridge width. Firstly, an EIL Qdash LD based comb source was realized by locking a single mode at 1609.47 nm and generating its harmonics with 50 GHz mode-spacing, as shown in Fig. 12(a) [42], [43]. The comb exhibited 7 lines with three central lines exhibiting an OSNR of 30 dB. The Lorentzian-fitted optical linewidths of the central three channels were ∼45 kHz. A drastic reduction in the optical linewidth was observed compared to the free-running Qdash LD mode measured in a few tens of MHz range before injection locking. Similarly, the phase noise of these channels was measured at a frequency offset of 1 kHz to be ~ -79 dBc/Hz. Next, the three-channel-comb signal was split into two halves where one half was utilized for modulation and transmission while the other unmodulated half was used as a LO at the receiver side, as depicted in Fig. 12(a). The first half was modulated via an MZM by a $2^{11} - 1$ long PRBS in a QPSK modulation scheme at a symbol rate of 32 Gbaud (64 Gb/s). Then, the modulated comb signal was dis-interleaved into even and odd parts and then decorrelated. After that, both odd and even modulated modes were recombined via another optical coupler, and the multiplexed signal was transmitted over a 10-km SMF. Fig. 12(b) shows the comb source's unmodulated de-interleaved odd and even modes at locations P3 and P4 alongside the recombined 32-Gbaud modulated signal at location P5 [42], [43]. A tunable filter was used at the receiver side to select the desired channel to be received at an OMA. Simultaneously, the matching mode of the unmodulated comb was filtered by another OBPF to be used as a corresponding LO. The OMA then performed coherent detection and post signal processing to recover the modulating signal. As such, all three channels showed a BER below the FEC threshold, with the transmission results of the left and central channels shown in Figs. 12(c) and (d), respectively. Thus, an aggregate data rate of 192 Gb/s (3 × 64 Gb/s) with a net spectral efficiency of 1.2−1.8 b/s/Hz was reported.

V. QUANTUM DASH LASERS IN FREE SPACE OPTICAL COMMUNICATIONS

Optical wireless communication has also been recognized as a promising supplement to existing fiber-optic networks, providing large bandwidth and high data rates, thus complementing the goals of NG-PONs, besides exhibiting nominal CapEx and OpEx. FSO communication architectures rely on the line-of-sight principle and could be deployed in indoor and outdoor environments for last-mile access solutions. Thus, it is highly attractive, not to mention a license-free spectrum and seamless integration with the existing optical fiber network infrastructure. In literature, different demonstrations of Qdash LD based FSO in outdoor building-to-building communication, indoor data centers for intra/inter-rack communication, and radio over FSO have been reported, corroborating its viability as a versatile candidate light source for NG-PONs. In the subsequent sub-sections, a brief survey of FSO communication demonstrations based on C-band and L-band Qdash LDs as a light source is discussed and summarized in Table 2 in chronological order with achieved data rates illustrated in Fig. 1(b).

TABLE 2. Summary of the implementation of quantum dash lasers in FSO communication in literature in a chronological order.

	Qdash Source	λ [nm]	BW [nm]	#Modes	RIN [dB/Hz]	Modulation Scheme	link	#Ch.	Data Rate [Gb/s]	Ref.
L-band	EIL	1625	10	20 w/ EIL	–	DP-QPSK	4 m IFSO	1	64/100	[76-78]
	SIL	1605	10	10 w/ SIL	–	DP-QPSK	5 m IFSO	1	128	[79]
	SIL	1610	11	10 w/ SIL	–	DP-QPSK	10 m IFSO	1	176	[80]
	SIL	1615	10	11 w/ SIL	–	DP-QPSK	10 km SMF-16 m IFSO	1	176	[81]
	SIL	1615	10	11 w/ SIL	–	16QAM	11 km SMF-8 m IFSO	1	32	[74]
	SIL	1615	10	11 w/ SIL	–	DP-QPSK	22 km SMF-8 m IFSO	1	128	[75]
C-band	SIL+MLL	1550	–	8 w/ SIL	< -140	PAM-4	555 m OFSO	8	8×11	[82]
	SIL+MLL	1550	–	4 w/SIL	–	16QAM*	50 km SMF-500 m OFSO	1	10	[92, 93]

*OFDM-based, IFSO: Indoor FSO, OFSO: Outdoor FSO.

A. L-BAND FSO TRANSMISSION

The first demonstration of a FSO communication system employing a Qdash LD was in [76] that utilized a mid L-band Qdash LD of reference [71] with an EIL assisting scheme. The emission of the 4×800 μm^2 ridge waveguide FP laser diode was centered in the far L-band at ∼1625 nm with a 3-dB bandwidth of 9 nm. Using a commercial tunable single-mode master laser, EIL was carried out to injection-lock a single mode, with a locking tuning range of 20 nm from 1612 to 1632 nm, corresponding to 40 FP longitudinal modes with an SMSR of 36 dB. The injection locking and experimental transmission setup were similar to Fig. 10(b) except that the channel is a 4 m long indoor FSO link, consisting of two fiber collimators, each serving as FSO transmitter and receiver for free-space transmission of the collimated laser beam. The fiber collimator had a 3.6 mm-beam diameter, a beam divergence of 0.032°, and a focal length of 18.75 mm. The power loss of the 4 m FSO link was 1.5 dB, ascribed to the collimators' manual dual-axis alignment. Nevertheless, 64 Gb/s DP-QPSK modulated signal was successfully received and detected with a BER floor of 10^{-5} and a receiver sensitivity of −19 dBm. These results were soon improved and expanded upon in [77], [78] with an increased data rate of 100 Gb/s (25 Gbaud) over two FSO links of 2 m and 4 m lengths, exhibiting BER below FEC threshold. It was pointed out that the system does not employ any EDFA for optical amplification, and hence the link lengths were restricted. With the fine alignment of the fiber collimators, while engaging EDFA in the system, longer indoor and outdoor FSO links could be established. Furthermore, the obtained BERs were found to increase with increasing the misalignment of the optical beam such that a maximum tolerable beam displacement of 1.6 mm was estimated to maintain BER at the FEC threshold.

Later, instead of EIL, SIL was adopted in [79] as an assisting technique for stabilizing the performance of the Qdash LD. The SIL setup was identical to references [9], [73] discussed earlier and shown in Fig. 11(a). The Qdash LD had a cavity length of 600 μm and a ridge width of 3 μm with an FSR of 70 GHz. By employing an OBPF, a self-locking mode tunability of 6 nm was demonstrated in the wavelength range of 1600−1607 nm, with an SMSR of 30 dB and an average mode power of 10 dBm. In this experiment, the SIL mode was modulated with a PRBS of a length of $2^{11} - 1$ in a DP-QPSK scheme at a symbol rate of 32 Gbaud (128 Gb/s) and then transmitted over a 5 m indoor FSO link comprised of two fiber collimators and a mirror with a total channel loss of 4 dB. The signal was then coherently detected and processed by OMA. The results showed that a minimum injection ratio of −21.5 dB, corresponding to a self-injected mode power of 8.5 dBm and SMSR of 25 dB, was required for attaining BERs below the FEC threshold. Moreover, a minimum receiver sensitivity of −16 dBm ascertained BER above FEC operation. Lastly, The Qdash LD's spatial power density emitted in free space was also estimated to be ∼4.9 mW/cm^2 by considering maximum transmitted peak power of −3 dBm. This value was shown to be <0.1 W/cm^2 IEC 60825-1 standard limit for Class 1 laser classification for distances less than 100 m, thus qualifying the Qdash LD operation to be eye-safe under all conditions of normal use. Soon after, 44 Gbaud (176 Gb/s) DP-QPSK was successfully demonstrated in [80], [81], by employing SIL on the same Qdash LD in an extended indoor FSO link of a length of 10 m, showing a receiver sensitivity of −12 dBm to attain BER below FEC limit of 3.8×10^{-3}.

Lastly, a 16 m long indoor FSO link in addition to two FSO/SMF hybrid transmission links (H1: 11 km SMF-8 m FSO, and H2: 11 km SMF-8 m FSO-11 km SMF) was demonstrated [74], [75] on SIL mid L-band Qdash LD, as shown in the utilized experimental setup in Fig. 13(a). With the aid of SIL, particularly by tuning the pass window of the OBPF, any of the available18 modes over a tuning range of 11 nm (∼1602–1613 nm), with 0.6 nm-mode spacing (70 GHz FSR), could be self-injection locked as depicted in Fig. 13(b). Such tunability with OIL would potentially allow SIL Qdash LDs to be deployed as unified transmitters to serve multi-subscribers, where each locked mode serves as a subcarrier in the CO or colorless source for different ONUs in WDM-PONs. Nevertheless, after locking one of the available FP modes, the locked signal was modulated at a symbol rate of 32 Gbaud in DP-QPSK format (128 Gb/s) and transmitted through a 16 m indoor FSO link comprised of two SMF collimators and a broadband mirror. Fig. 13(c) shows the obtained BER as a function of the received power

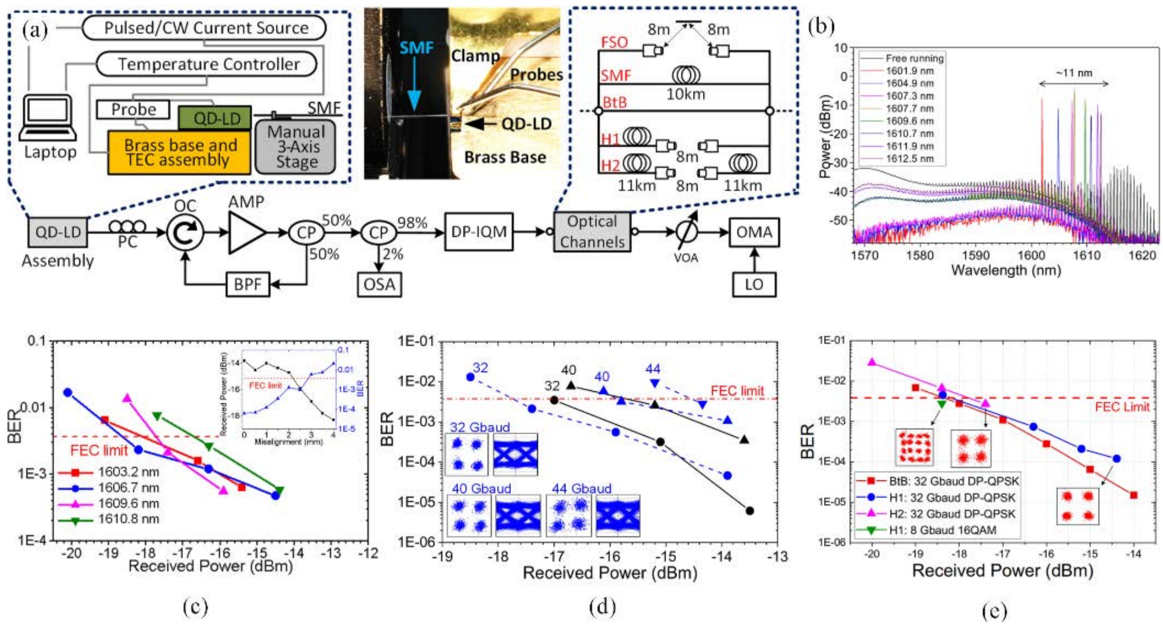

FIGURE 13. (a) The implemented experimental hybrid SMF-FSO-SMF transmission setup demonstrated in [74], [75] employing mid L-band Qdash LD. (b) Emission spectrum of different self-injection-locked FP modes from the Qdash LD emission spectrum. BER as a function of the received power for (c) 16 m FSO link employing 4 individual subcarriers, (d) 16 m FSO link with different symbol rates in DP-QPSK transmission at a fixed 1609.6 nm subcarrier, and (e) the two hybrid FSO-SMF links.

at the OMA for four different locked modes within the tuning window, serving as subcarriers, exhibiting below the FEC limit. After that, other data modulation rates were also investigated, namely, 32, 40, and 44 Gbaud (128, 160, and 176 Gb/s) for a fixed subcarrier at 1609.6 nm. Fig. 13(d) depicts the transmission performance wherein all the modulated signals reached BER below the FEC threshold with receiver sensitivities of −17 (128), −16 (160), and −14.5 dBm (176 Gb/s). In other words, up to 176 was demonstrated on the 16 m-indoor FSO link with spectral efficiency of 3 b/s/Hz. In terms of collimator misalignment effect, a maximum misalignment tolerance of 2.8 mm with −17.5 dBm received power was essential for maintaining a BER below the FEC limit. This translates to a beam-area misalignment of 60% at the receiver end (neglecting the beam diffraction). Next, the two hybrid SMF/FSO transmission links were investigated, emulating the scenario where two distant SMF networks inter-connected via FSO links, e.g., racks within data centers. Fig. 13(e) shows the measured BER for both hybrid channels [74], [75]. In both configurations, DP-QPSK was adopted as a modulation scheme at a rate of 32 Gbaud (128 Gb/s), and both exhibited a similar receiver sensitivity of −18 dBm to attain below FEC-limit operation. In addition, 16QAM was also attempted as a higher-order modulation format for the first time over a mid L-band Qdash LD at a symbol rate of 8 Gbaud (32 Gb/s) through the first hybrid link, H1, where BER below FEC-limit was also attained.

B. C-BAND FSO TRANSMISSION

Implementation of C-band Qdash LD in FSO transmission was reported in [82] by employing a Qdash MLL in a WDM system with the aid of the SIL assisting technique, as shown in Fig. 14. The Qdash material was grown by gas source MBE on an S-doped (100) InP substrate, consisting of 9 layers of InAs Qdashes separated by InGaAsP barrier layers. The cleaved laser diode with a cavity length of 840 μm, translating to an FSR of 50 GHz to match the DWDM ITU's grid standard, was employed. In this work, SIL was employed to further improve the noise characteristics of the 1550 nm Qdash MLL, particularly RIN, which is a critical parameter in intensity modulation that was adopted in this work. It was shown that before SIL, the measured average RIN was −110 dB/Hz at low frequencies. However, this value drastically reduced for individually filtered modes and fell in the range of −155 to −140 dB/Hz after SIL. By tuning the OBPF used in the SIL loop, shown in Fig. 14(a) [82], 8 FP modes, with a mode spacing of 50 GHz, were extracted from the multi-wavelength emission of the Qdash MLL. Next, an AWG de-MUX with a matching 50 GHz-spacing was used to further increase the SMSR of the eight modes to 50 dB. In this experiment, the self-injection locked 8 modes were modulated via an MZM with a PRBS of a length of $2^{15} - 1$ in PAM4 format at a data rate of 11 Gb/s and encoded by a Reed–Solomon (528, 514) code. The modulated signal was then amplified via an EDFA and then transmitted over a 555 m long outdoor FSO link, comprised of two refractive telescopes, producing an approximately 24 mm collimated beam to prevent the system from diffraction. Nonetheless, at the receiver side, the signal was multiplexed via a 50 GHz/100 GHz optical interleaver into eight different channels, where odd and even optical sidebands are separated by adjusting the proper channel spacing of the interleaver. Then the particular desired channels of the optical carriers were filtered via tunable OBPF. Each channel

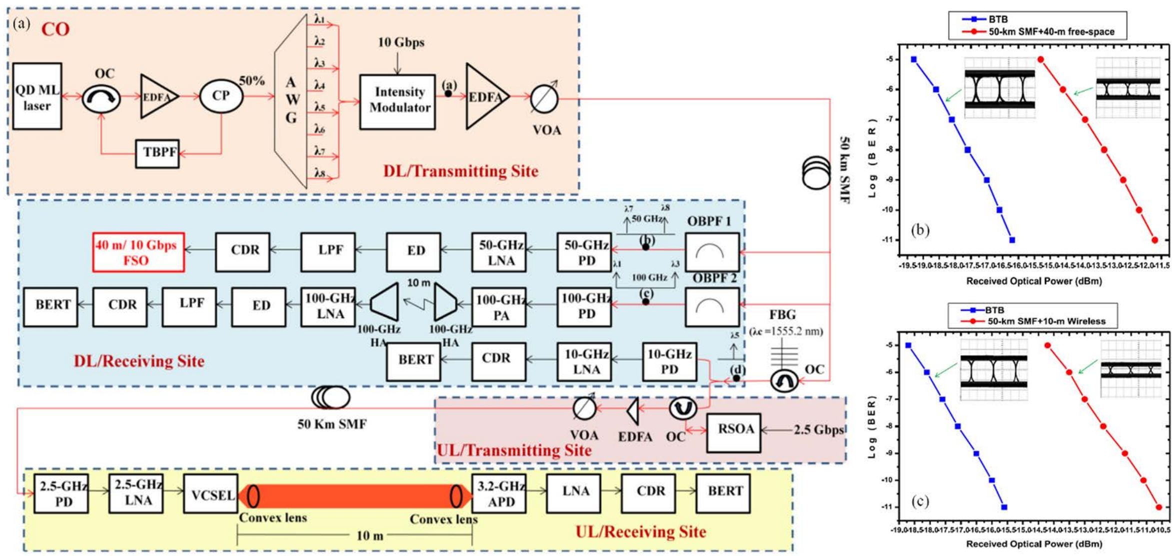

FIGURE 14. (a) The experimental hybrid SMF-WL-FSO communication system implemented in [70] and similar to [82] employing C-band Qdash LD. The measured BER as a function of the optical received power for (b) the 50 GHz signal transmitted in the 50 km SMF - 40 m FSO hybrid link and (c) the 100 GHz signal transmitted over the 50 km SMF - 10 m WL link [70], [82].

was then detected on a photodiode and decoded by a Reed–Solomon decoder, which was then passed to a digital storage oscilloscope (DSO) for storage and analysis. As such, all 8 signals showcased BER below the FEC limit, translating to an aggregate data rate of 88 Gb/s (8×11 Gb/s) with an average receiver sensitivity of -13 dBm and -9 dBm with and without implementing the Reed–Solomon codec scheme, respectively. In other words, a receiver sensitivity improvement of 4 dBm was attained by employing the Reed–Solomon code scheme.

VI. QUANTUM DASH LASERS IN MMW/THz BASED COMMUNICATIONS

Traditional electronic systems for MMW generation impede network scaling due to their high complexity, low spectral efficiency, and larger sizes, besides limiting the highest achievable frequency. In this regard, photonic generation and transmission of MMWs have been given considerable regard as a strong contender for 5G networks and their integration with the existing fiber infrastructure via RoF technology. This study of Microwave photonics has seen a sharp increase in the last few years, thanks to the envision of NG-PONs. Optical heterodyning has been the most researched approach in the literature for optical generation of MMW signals and relies on beating two optical wavelength carriers by a photodiode, a typical square-law detector. The two optical carriers could be extracted from a comb source, dual-wavelength laser, or could be from two separate free-running LDs. In general, it has been shown that deploying free-running LDs gives rise to broadened MMW beat-tone linewidths with high phase noise due to coherency-mismatch between them, or phase-mismatch. Therefore, techniques such as optical phase-locked loops and OIL have been employed on laser sources for successful spectral synchronization and purification of the heterodyned MMW carrier with ultra-narrow linewidth and low phase noise, which are paramount for high-performance transmission when employed as sub-carriers [83].

Due to improved static and dynamic characteristics exhibited by Qdash nanostructures, particularly noise feature, compared to the Qwell counterparts, Qdash LDs have been garnering attention as candidate light sources in the Microwave photonics domain. Besides, the niche feature of Qdash emission spanning emission wavelength from S- to L-band regions, Qdash LDs could serve as promising MMW sources in seamless integration with existing optical network infrastructure and satisfying the extended L-band wavelength operation in future optical and hybrid network architectures that are under serious consideration. Moreover, the multi-wavelength lasing emission feature of Qdash LDs could also be exploited in future MMW RoF-WDM systems, allowing a single device to supply dual optical carriers to multiple C- or L-band channels exhibiting either unique MMW beat-tone frequency carrier or different frequencies carrier.

This section discusses different MMW frequency carriers generation and communication demonstrations over WL and hybrid channels, employing Qdash LD from the literature, summarized in Table 3 and plotted in Fig. 1 (c). The reported works are categorized based on incorporating a WL channel in the system; with two sub-sections: first including WL channel link, *viz.* transmission over WL/hybrid SMF-WL/hybrid SMF-FSO-WL channels, and the second section discuss results that do not incorporate WL channel, *e.g.*, SMF/SMF-FSO channel transmission.

A. TRANSMISSION WITH WIRELESS LINK

The first demonstration of MMW generation and WL transmission using a Qdash LD was reported in [84]–[86] via a FP C-band Qdash MLL, with a self-pulsation frequency

TABLE 3. Summary of the implementation of quantum dash lasers in MMW transmission in literature.

Tx	Qdash Source	λ [nm]	MMW Beat Frequency	Δf	SNR [dB]	Modulation Scheme	Link	Data Rate [Gb/s]	Ref.
WL	MLL	C-band	60 GHz	18 kHz	30	OOK	25 m WL	5	[84-86]
	DFB	C-band	146 GHz	700 kHz	28	OOK	2.5 cm WL	1	[88]
	SIL+MLL	C-band	100 GHz	16 kHz	30	OOK	50 km SMF-10m WL	10	[70]
	SIL+MLL	C-band	40/80 GHz	–	40	16QAM*	50/25 km SMF-20 m WL	10	[92, 93]
	SIL	L-band	28/38/60 GHz	–	30	–	6 m WL	–	[97]
	DFB	C-band	47 GHz	41 kHz	–	64QAM	25 km SMF-4 m WL	24	[95]
	EIL/SIL	L-band	28 GHz	few kHz	36	QPSK	20 km SMF-5 m FSO-6 m WL	2	[44,98]
	SIL	L-band	30 GHz	few kHz	28	QPSK	20 km SMF-5 m FSO-2 m WL	2	[45]
	MLL	C-band	25 GHz	3 kHz	–	16QAM	25 km SMF-2 m WL	16	[96]
	SIL	L-band	25/28 GHz	–	–	16QAM	10 km SMF-4 m WL	8	[99]
No WL	MLL	C-band	60 GHz	10 kHz	–	QPSK*	50 m SMF	3	[100]
	SIL+MLL	C-band	50 GHz	16 kHz	30	OOK	50 km SMF	10	[70]
	SIL+MLL	C-band	60 GHz	50 kHz	50	64QAM*	25 km SMF	1.12	[102, 103]
	DFB	C-band	47 GHz	41 kHz	–	PAM4	BtB SMF	2	[64]
	SIL+EIL	C/L-band	60 GHz	–	40	32QAM*	50 km SMF-100 m FSO	6.5/10	[104]
	SIL+EIL	C/L-band	1.1/1.3 THz	–	40	32QAM*	25 km SMF-100 m FSO	10/12.5	[104]

* OFDM-based, Tx: Transmission channel including WL sub-link and with no WL sub-link, Δf: RF 3dB linewidth, λ: Wavelength window operation

of 60 GHz, corresponding to the inverse of the round-trip time of the optical wave in the 710 μm long cavity. The Qdash MLL emitted at 1570 nm with a 3-dB bandwidth of 10 nm. The generated MMW was based on the heterodyne beating of neighboring two modes out of the signature comb lines of Qdash MLLs, resulting in a beat-tone of frequency equal to its FSR. First, the comb of Qdash MLL was modulated with the OOK modulation scheme at a data rate of 5 Gb/s via an electro-absorption modulator by a PRBS of a length of $2^{31} - 1$. The modulated signal that includes the entire broadband lasing spectrum was transmitted over a 50 m SMF and then detected by a 70 GHz photodetector, thus detecting the 60 GHz MMW carrier without any side harmonics. The RF signal was then amplified and transmitted in a 25 m long outdoor WL link consisting of two 23-dBi horn antennas. Fig. 15 (a) depicts the experimental transmission setup, while Fig. 15 (b) plots the measured BER after detection and recovery for different data rates, showing successful transmission [84]–[86].

Soon after, two monolithically integrated 1550 nm distributive feedback (DFB) Qdash LDs were utilized in [87] to generate MMW signals. In this configuration, dual-mode emission was demonstrated from the twin Qdash DFB laser, where the mode spacing could be tuned by independently biasing each of the DFB sections with a tuning range of 3 to 20 GHz and exhibiting RF linewidths <1.0 MHz. The work was subsequently extended in [88] with similar twin Qdash DBF LDs displaying beat-tone frequency tuning range from 70 to 146 GHz, with an SMSR between 28-34 dB. A dual 146 GHz beat tone was generated and externally modulated by a 2^7-1 PRBS in OOK format at a data rate of 1 Gb/s by MZM. Then, the modulated optical signal was amplified and opto-electronically converted via a packaged high-speed antenna-integrated traveling-wave uni-traveling carrier photodiode, integrated with a broadband log-periodic antenna of a gain of 20 dBi and 2.5 cm distance over the air from the transmitter to receiver. Thus, the received signal showed an eye-opening of 723 ps in the best case. Later reports on C-band Qdash MLL were towards either generation of MMW equivalent to the FP cavity FSR [89] or deployment in non-linear phenomena applications [90] [91]. For instance, Qdash MLL was utilized in [90], where the comb of the 100 GHz FSR was used with a frequency-selective filter to provide two tunable wavelength pumps for wavelength conversion of optical channels in a dual-pump four-wave-mixing scheme. After a few years, the following report came by exploiting Qdash MLL emitting in the C-band at ~1543 nm with a 3-dB bandwidth >10 nm and exhibiting FSR of 33.6 GHz [91]. This work used Qdash MLL as a dual pump source for a wavelength conversion system. Next, another Qdot/Qdash MLLs were reported in [89], comprised of five layers and emitting in the C-band. By beating any consecutive modes of the comb lines of the Qdash MLLs, a high-quality beat tone of 34.46 GHz was generated.

A WDM hybrid SMF-WL-FSO demonstration was also reported in [70], whose experimental setup was shown in Fig. 14(a). As discussed in the previous section, SIL locking was implemented over a C-band Qdash MLL identically to [82] to lock 8 modes from which 5 high-quality comb carriers were chosen for the WDM optical transmission where they were modulated via a MZM at a data rate of 10 Gb/s with OOK, amplified and transmitted through a 50-km SMF. Later, as illustrated in Fig. 14 (a), the 100 GHz (λ_1, and λ_3) and 50 GHz MMW (λ_7 and λ_8) MMW downlink beat-tone received optical signals, which were obtained via an optical coupler and appropriate OBPF, were beaten separately over photodiodes, and then amplified via a low-noise amplifier. The resulting RF 50 GHz signal showed a linewidth of 16 kHz, was down-converted by an envelope detector, and was fed to a 40-m long FSO link, comprised of a directly

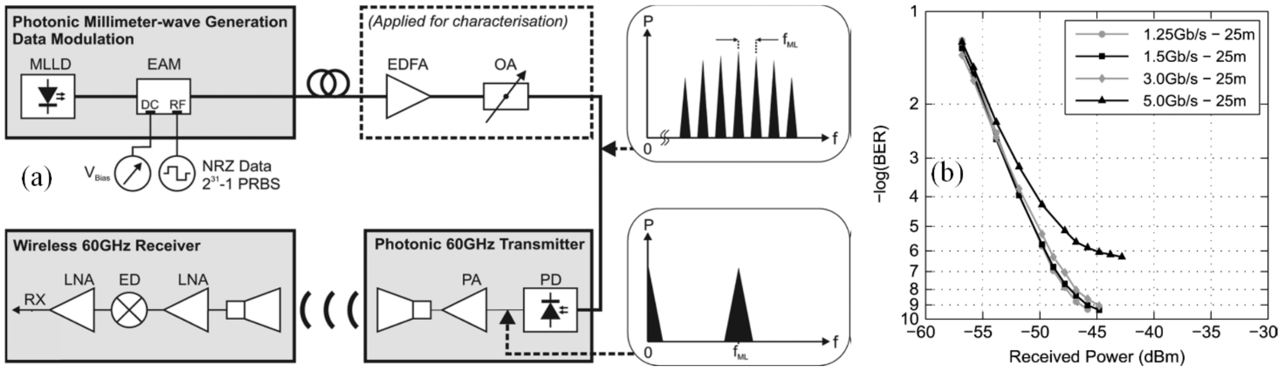

FIGURE 15. **(a) The experimental MMW wireless communication system implemented in [84]–[86] employing C-band Qdash MLL, with an inset depicting the optical spectrum before photodiode and electrical spectrum after photodiode. (b) The measured BER as a function of the optical received power at different data rates for the SMF- 25 m WL channel.**

modulated DFB laser diode as a transmitter, and a pair of identical FSO terminals with fine tracking technology. On the other hand, a 100 GHz MMW electrical signal also displayed an RF linewidth of 16 kHz, transmitted through a 10-m WL link comprised of two 100-GHz horn antennas with a gain of 25 dBi. The transmitted signal was then down-converted by an envelope detector and then passed for clock/data recovery and BER testing. Fig. 14 (b) and (c) shows the measured BER as a function of the received optical power for the 50 GHz and 100 GHz MMW signals which were transmitted through the 50-km SMF - 40-m FSO link and 50 km SMF - 10 m WL link, alongside the BtB case, respectively [70]. A receiver sensitivity of −13 (−12.21) dBm and a power penalty of 4.3 (4.8) dB is reported when compared to the BtB link at a BER of 10^{-9}. This was attributed mainly to the fiber dispersion after the 50-km SMF transmission and FSO power loss for the 50 GHz case and the fading effects over the WL channel for the 100 GHz signals. Soon after, this work was expanded in references [92], [93], using the same 1550 nm Qdash MLL and SIL. Out of its broad emission, 4 modes were selected in a similar manner with 100 GHz spaced AWG, which were then modulated via an MZM by a 10 Gb/s orthogonal frequency division multiplexed (OFDM) data stream in 16QAM format. The modulated comb signal was then transmitted through a 50 km SMF and again phase modulated by a 20 GHz RF signal source to generate side harmonics for each of the 4 modes. Then an optical dis-interleaver was used to separate the odd and even sidebands. As a result, two MMWs were generated, *viz.* 40 GHz and 80 GHz from the odd and sidebands, respectively. The 40(80) GHz MMW was then transmitted through a 50(25) km SMF followed by a 20 m WL link comprised of two horn antennas. As such, both transmission links exhibited a BER < FEC threshold of $3.8 \times 10^{-3,}$ indicating successful communication. Furthermore, the 80 GHz MMW was also successfully transmitted through a 50 km SMF and 500 outdoor FSO hybrid link instead of the WL link, exhibiting BER less than the FEC threshold.

Later, in [10], a buried heterostructure dual-wavelength DFB Qdash LD was realized on a single 1.8 mm long cavity and exploiting a novel synthesized aperiodic non-uniform diffraction grating layer placed below Qdash active layer. The device simultaneously generated two coherent optical modes at ∼1540 nm, as depicted in Fig. 16(a) [10], with spectral linewidths as narrow as 15.8 kHz. The spacing between the dual modes could be tuned between 46 and 48 GHz, whereas the average RIN was measured to be −151 dB/Hz over the frequency range of 10−20 GHz. The device was later utilized in [64], [94] to generate a 47.2 GHz-MMW, which was modulated via an MZM in a PAM4 modulation scheme at a symbol rate of 1 Gbaud (2 Gb/s). The generated MWW exhibited a 3-dB RF linewidth of 41 kHz. The MMW signal was then transmitted in a BtB and SMF configuration to be captured by a RTO, which showcased an open eye diagram for the recovered 2Gb/s-PAM4 MMW signal. Later, the same device was employed in [95], where the 47-GHz MMW signal was instead modulated at a symbol rate of 4 Gbaud in 16QAM, 32QAM, and 64QAM modulation schemes. The MMW signal was then transmitted through a hybrid link consisting of a 25.22 km SMF and 4-m WL channel, as shown in Fig. 16(b) experimental setup. As such, below FEC limit results were obtained, as depicted in Fig. 16(c), which shows the measured error-vector-magnitude (EVM) as a function of the received power for the 16QAM signal. On the other hand, Figs. 16(d) and (e) depict the constellation diagram for the 32QAM and 64QAM signals, respectively [95].

In reference [96], a C-band Qdash MLL comprised of 5 stacks of InAs Qdashes active region was cleaved at a cavity length of 1735 μm, corresponding to an FSR of 25 GHz. The Qdash MLL emitted at 1531 nm with a 6-dB bandwidth of 9 nm comprising 47 comb lines with an OSNR > 40 dB. The RIN of individual modes was measured between −130.7 and −136.6 dB/Hz over a frequency range of 10 MHz to 20 GHz. The optical linewidth of the comb lines was found to be between 150 and 300 kHz, whereas the RF linewidth resulting from beating two consecutive modes was found to be <3 kHz. The photonic generation of the MMW in this work was carried out by filtering two adjacent comb lines 1533.044 nm (λ_1) and 1533.240 nm (λ_2), using two OBPF, exhibiting optical linewidths 167.8 kHz

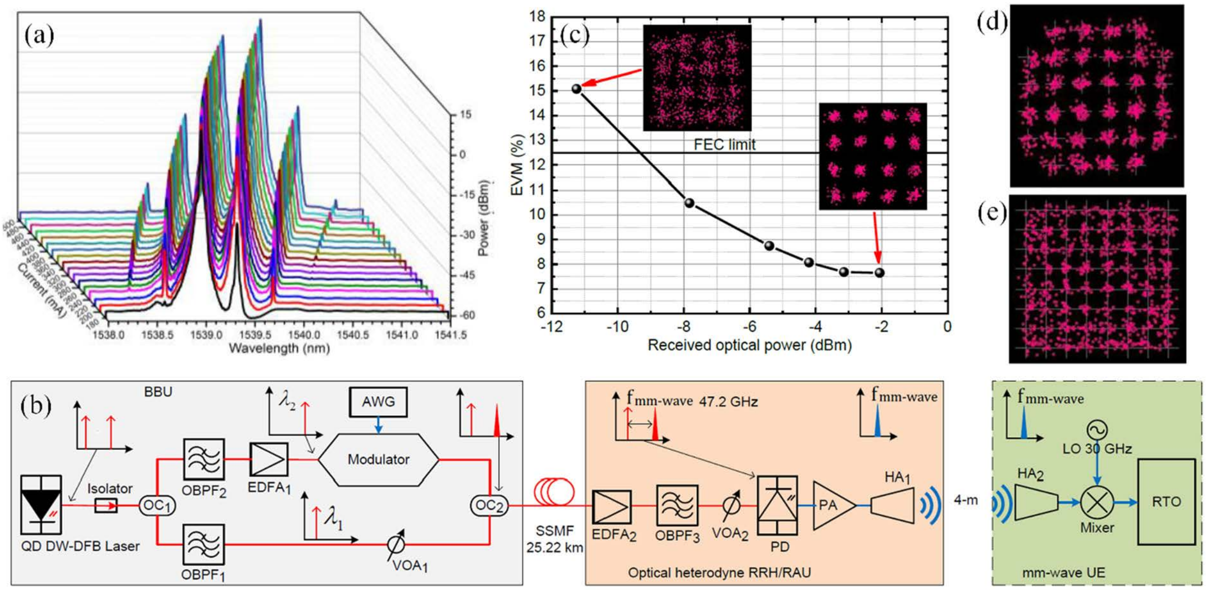

FIGURE 16. (a) Dual-mode emission of the DFB Qdash LD demonstrated in [10], [64], [94], and [95] (b) The implemented experimental hybrid 25.22-km-SMF - 4 m WL communication system implemented in [95]. (c) The measured EVM as a function of the received power for the 16QAM MMW signal. The constellation diagram for the 4 Gbaud (d) 32QAM and (e) 64QAM signals.

and 141.8 kHz, and integrated RIN −134.384 dB/Hz and −136.655 dB/Hz, respectively. After that, the shorter wavelength mode was modulated by a PRBS of a length of $2^{11} - 1$ in 16QAM format at a symbol rate of 4 Gbaud (16 Gb/s) and then combined with the unmodulated longer wavelength mode to be transmitted over a 25 km SMF. The received optical MMW beat-tone at the remote radio unit was beaten together on a fiber-optic receiver to generate a 25.09 GHz MMW signal. The MWW signal was then transmitted over a 2 m WL link consisting of two 20-33 GHz horn antennas with a gain of 17 dBi. Then at the receiver side, the signal was amplified by a low noise amplifier and then captured on a RTO for analysis. The BER of the received signal was less than the FEC limit with an EVM of 8.43% and a BER of 1.3×10^{-5}.

The first MMW WL transmission incorporating a mid L-band ∼1610 nm Qdash LD was reported in [97]. The work employed the SIL scheme discussed in [74], [75] and utilized an identical device structure with a cavity length of 800 μm and a ridge width of 3 μm. The SIL mode was then employed to realize SIL Qdash LD based comb source with different mode spacings *viz.* 28, 38, and 60 GHz. Later, three corresponding frequency MMW beat-tones were generated by filtering two comb lines via an OBPF in each case. After that, each MMW beat-tone, acting as a subcarrier, was transmitted wirelessly for a few meters without modulation and was received and analyzed over an electrical signal analyzer (ESA). In terms of the phase noise, a noise floor was measured as −118 and −105 dBc/Hz after the 2 m and 6 m WL links, with measured RF line width in the sub-kHz range.

The same team recently extended their work by demonstrating the transmission of a modulated 28 GHz MMW over a hybrid SMF-wireless link with the aid of a mid L-band EIL Qdash LD based comb source [44]. Fig. 17(a) shows the implemented experimental setup. The photonic generation of the 33 GHz MMW was carried out similarly to that in [74], [75]. The two filtered modes from the comb source are shown in Fig. 17(b), exhibiting 33 GHz spacing. Afterward, the dual modes were modulated by a $2^{11} - 1$ long PRBS at a data rate of 2 Gb/s in QPSK format. The baseband analog QPSK was offset to an intermediate carrier frequency of 5 GHz, thereby essentially translating to a 28 GHz beat tone. Next, the 28 GHz beat tone signal was amplified and transmitted through a 20 km SMF, which was then detected over a 70-GHz bandwidth photodiode to beat the two modes and generate the 28 GHz MMW, which was then amplified and transmitted through a 0−4 m WL channel comprised of two horn antennas of 25 dBi gain. The received electrical MMW signal from this hybrid 20 km SMF and 4 m WL channel was then down-converted, demodulated, and analyzed in a digitizer. The measured phase noise at a frequency offset of 1 MHz for the 28 GHz modulated MMW and the unmodulated 33 GHz MMW carrier displayed values of ∼ −116 dBc/Hz at the transmitter side and degraded to ∼ −109(−100) dBc/Hz after the 20 km SMF-2 m WL (20 km SMF-4 m WL) transmission. Nevertheless, the RF linewidth of both MMW signals was measured to be between a few kHz to the sub-kHz range. Next, Figs. 17(c) shows the transmission performance of the 28 GHz MMW carrier over the two hybrid-channel links in terms of EVM [44]. Both transmission experiments yielded an EVM less than 37%, corresponding to the FEC limit, with a receiver sensitivity of −4.5 and −1 dBm, for the 2 and 4 m WL links of the hybrid SMF-WL channel, respectively.

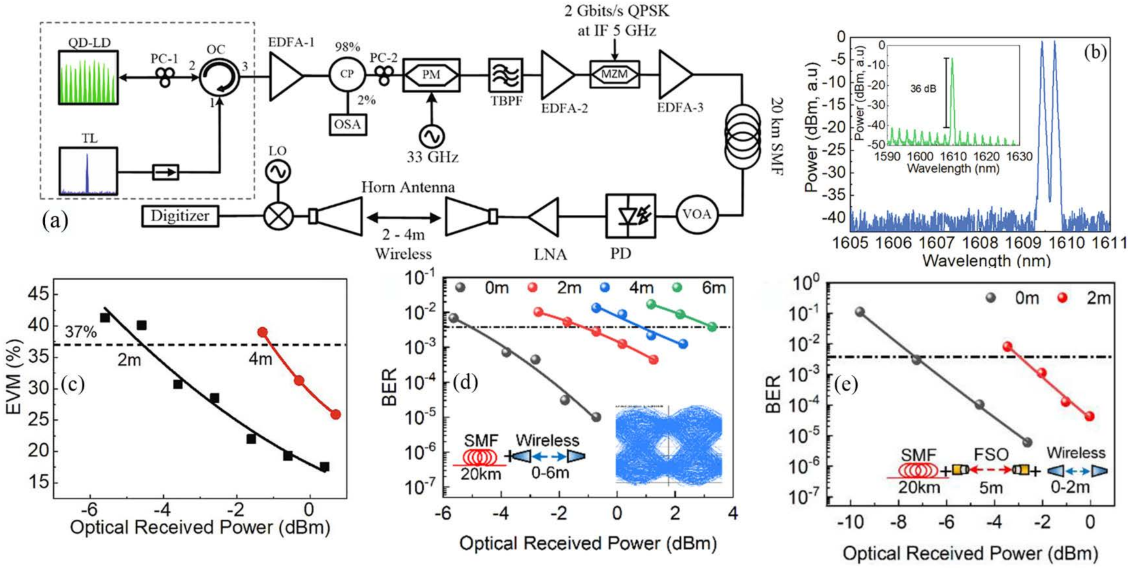

FIGURE 17. **(a) The hybrid 20 km SMF - 2-4 m WL communication system employing mid L-band EIL Qdash LD based comb source [44]. (b) The extracted two modes of the comb source with 33 GHz mode spacing and the EIL mode in the inset. (c) Performance of the 28 GHz MMW over the 20 km SMF- 2-4 m WL hybrid links in terms of EVM. Performance of (d) 28 GHz MMW SIL Qdash LD based comb source over 20 km SMF - 0-6 WL transmission channel [45], and (e) 30 GHz MMW SIL Qdash LD based comb source over 20 km SMF - 5 m FSO - 0-2 WL transmission channel [45]. The inset of (d) shows the eye diagrams at ∼0 dBm received power for 0 m WL distance.**

Soon after, another MMW transmission demonstration was reported in [45] employing SIL Qdash LD based comb source emitting in the mid L-band. Two neighboring lines at ∼1610 nm from the 33 GHz spaced comb were filtered and then modulated with 1 Gbaud QPSK (2 Gb/s) at an intermediate carrier frequency of 5 GHz, resulting in a modulated 28 GHz MMW beat-tone. Similarly, another modulated 30 GHz MMW beat-tone was also generated from a 35 GHz spaced SIL Qdash LD based comb source. In this work, hybrid. 20 km SMF- 6 m WL and 20 km SMF - 5 m FSO-2 m WL transmission channel performance were evaluated. The generated 28 GHz MMW beat-tone was utilized in the transmission experiment with the former hybrid channel, and the results are depicted in Fig. 17(d) [45]. The BER below FEC was measured for various WL link lengths with a minimum required optical power of 0.7 dBm for the 4 m WL link case. On the other hand, the modulated 30 GHz MMW beat-tone was transmitted through the latter hybrid channel, with the corresponding measured BER shown in Fig. 17(e) [45]. Below FEC BER was obtained at a receiver sensitivity of −3 dBm for the 2 m WL sub-link. It was noted that despite experiencing a longer transmission channel, the receiver sensitivity exhibited a smaller value in the BtB configuration when compared to the 28 GHz MMW system counterpart. This was ascribed to the frequency-dependent chromatic-dispersion-induced power fading of the MMW beat tones while propagating through the SMF. Moreover, the work was extended to study the effect of dust storm climate conditions on the performance of 2 Gb/s QPSK modulated 30 GHz MMW beat-tone over 20 km SMF −1 m FSO −1 m WL channel [98] in terms of visibility. After a comprehensive analysis employing both EIL and SIL Qdash LD based comb sources, the required visibility of ∼14 m was measured from both sources to satisfy the EVM and BER FEC limit of successful transmission.

Lately, a hybrid bi-directional SMF-WL MMW transmission was demonstrated in [99] via a mid L-band Qdash LD emitting at 1610 nm. Fig. 18(a) shows the experimental setup of the system. The SIL Qdash LD based comb source was utilized to filter two modes with 28 GHz spacing serving as optical carriers for upstream transmission through the shorter wavelength and downstream transmission over the longer wavelength modes, as shown in Fig. 18(b). The dual modes were separated, and the downstream carrier was modulated with data before combing with the unmodulated upstream optical carrier and transmitted over a 10 km SMF. The downstream optical carrier was modulated at a data rate of 8 Gb/s in the QPSK format. The downstream MMW beat-tone was then converted into an electrical signal at the remote access unit (RAU) and then transmitted through a 4 m WL link using a pair horn antenna before being received and analyzed at a remote radio head unit (RRH). For the upstream path, the 8 Gb/s QPSK or 16QAM modulating signal was up-converted over 25 GHz MMW carrier and then transmitted through to the RAU via a 4 m WL link. Then, the RF signal was converted into the optical domain by intensity modulating the upstream optical carrier that was available from the downstream signal after passing through a 3-dB coupler. The upstream MMW beat-tone was then transmitted through the same 10 km SMF utilized for downstream

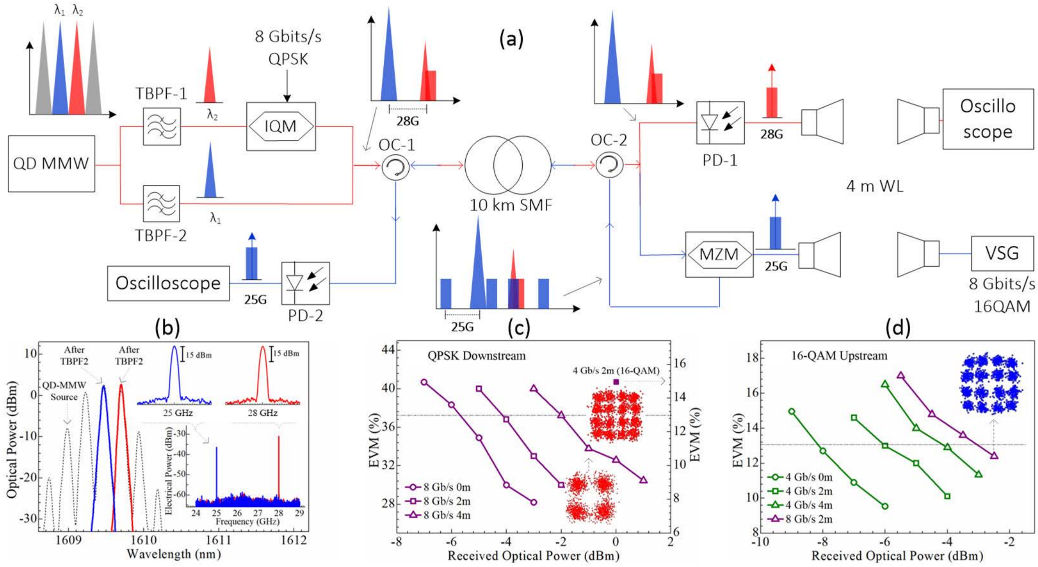

FIGURE 18. (a) The implemented 8 G/s QPSK downstream and 16QAm upstream experimental setup of the bidirectional hybrid 10 SMF- 4 WL MMW transmission employing mid L-band SIL Qdash LD based comb source [99]. (b) The emission spectrum of the comb source with the extracted two modes and insets shows the 28 GHz downstream and 25 GHz MMW signals. (c) QPSK downstream and (d) 16-QAM upstream performance with the constellation shown for the indicated received powers.

signal transmission. The successful simultaneous transmission was attained for both 28 GHz downstream and 25 GHz upstream signals, evident by the BER and constellation diagrams shown in Figs. 18(c) and (d), respectively [99].

B. TRANSMISSION WITHOUT WIRELESS LINK

The first RoF transmission without WL sub-link was demonstrated in [100] and later followed by [101], where a C-band Qdash MLLs consisting of 9 stacks of InAs Qdash-in-well structure was utilized with different cavity lengths, corresponding varying repetition rates or FSR from 24 – 209 GHz, and measured RF linewidths as low as 10 kHz for 50-60 GHz FSR devices. In particular, a 780 μm long Qdash MLL was selected for direct generation of a MMW tone at 55 GHz. Then, the signal is up-converted to 60 GHz with intermediate frequency by an in-phase quadrature mixer. The signal was modulated at 3 Gb/s in QAM in BtB RoF link with EVM of 11%. The next RoF transmission demonstration was in the previously-discussed duplex SMF-WL system reported in [70] and shown in Fig. 14, where a 50 GHz MMW manifested by beating λ_7 and λ_8 out of the eight comb lines of the utilized Qdash MLL emitting in the C-band.

Later, in references [102], [103], optical feedback was utilized with a C-band Qdash MLL in an optical heterodyne RoF system. The comb emission of the Qdash MLL exhibited a repetition rate of 32.5 GHz with a beating RF linewidth of tens of kHz and a 3-dB bandwidth of 11.8 nm, while the average mode optical linewidth was 6 MHz. An optical external free space cavity, consisting of a collimating lens, a free space attenuator, and a mirror, was used to provide feedback in the form of free-space SIL. Two 65-GHz apart modes were selectively filtered out of the Qdash MLL's emission comb via a wavelength selective switch for heterodyning. Next, an OFDM signal was generated via an MZM at an intermediate frequency of 5 GHz, with 64QAM format, creating two optical tones at 60 and 70 GHz, at a symbol rate of 1.95 Mbaud (1.12 Gb/s). Then, the modulated signal was combined with an unmodulated copy and transmitted through a 25 km SMF. As such, a measured BER of 10^{-4} <FEC-limit was obtained with no penalty due to fiber transmission at a received optical power of 0 dBm.

Very recently, in reference [104], two Qdash LDs were employed with the aid of both EIL and SIL to realize an OFDM-based bi-directional MMW-over-fiber and THz-wave-over-fiber transport system. One Qdash LD emitted in C-band between 1554 to1562 nm, and the other in L-band from 1600 to1620 nm. In this work, the C-band Qdash LD was dedicated for uplink transmission, while the L-band Qdash LD was used for downlink transmission. Both EIL and SIL are implemented to lock one mode each out of the broad lasing for each laser device, as illustrated in Fig. 19 (a). This MMW/THz beat-tone generation technique was first introduced in [105] over an L-band Qdash LD. Nevertheless, as shown in Fig. 19 (b) [104], by adequately tuning the utilized OBPF in the SIL loops and the emission of the tunable laser in EIL, different beat tones were obtained with an SMSR ~40 dB as: 60 GHz and 1.3 THz over the C-band Qdash LD, and 60 GHz and 1.1 THz over the L-band Qdash LD. In each of the four cases, each dual-mode tone was modulated in OFDM with 32QAM format at different data rates for each of the four-beat tones as follows: 10 Gb/s for the downlink L-band 60 GHz MMW, 6.5 Gb/s for the

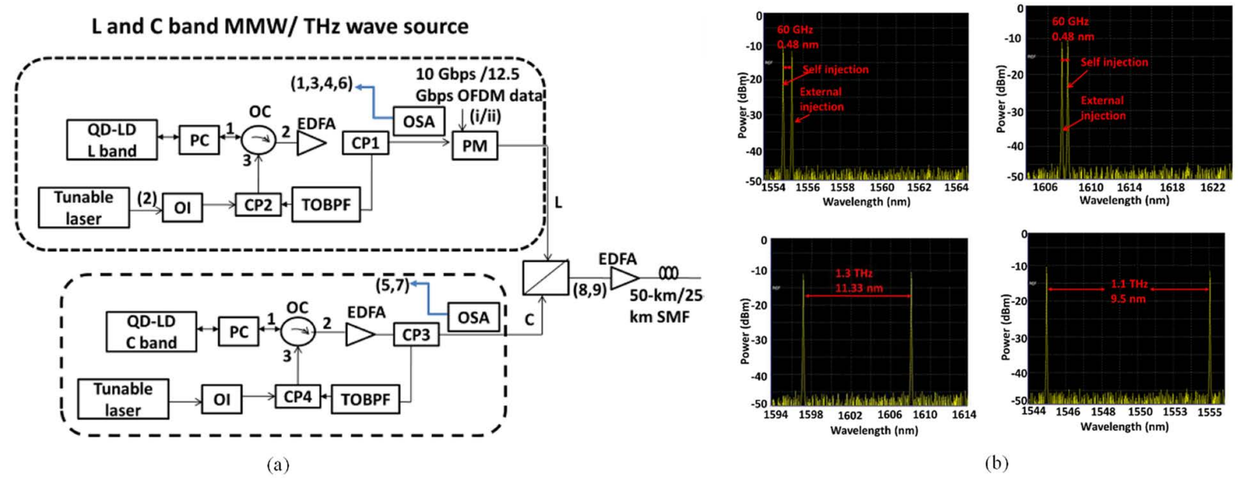

FIGURE 19. (a) The implemented experimental setup employing both EIL and SIL for the photonic generation of the MMW/THz waves to be transmitted in the RoF link utilizing C-band and L-band Qdash LDs [104]. (b) Different optical spectra show two locked modes using SIL and EIL on both the C-band and L-band Qdash LDs to generate 60 GHz or THz beat tones.

uplink C-band 60 GHz MMW, 12.5 Gb/s for the downlink L-band 1.3 THz, and 10 Gb/s for the uplink C-band 1.1 THz carriers. The L-band downlink data stream was transmitted through a hybrid 50 km SMF/100 m FSO link for MMW signals. At the receiver side, the signal was fed into a RTO for analysis. On the other hand, the THz waves were detected by a zero-bias detector followed by a OBPF and was down-converted by a LO and a mixer, and then the data was recovered with the assistance of clock data recovery. Finally, the signals were fed into a BER tester to analyze their performance. On the other side, the uplink C-band data was routed through a separator and modulated to be transmitted through another hybrid 100 km SMF/100 m FSO link. With that said, all four MMW/THz signals were recovered successfully with BER below the FEC limit over the hybrid channel. For the MMWs, the receiver sensitivity was −18.5 dB and −16.1 dB for the downlink and uplink signals, respectively, with a corresponding power penalty of 4.5 dB. On the other hand, the associated receiver sensitivities with the THz signals were −17 and −16.5 dB for the downlink and uplink signals, respectively, with a corresponding power penalty of 2.3 dB.

5G	Fifth-generation
AFM	Atomic force microscopic
AMZI	Asymmetric Mach Zehnder interferometers
ASE	Amplified spontaneous emission
ASK	Amplitude shift keying
AWG	Array waveguide grating
BER	Bit-error rate
BPS	Blind phase search
BRM	Bit rate multiplier
BtB	Back-to-back
CaPEx	Capital expenditure
CO	Central office
DCF	Dispersion compensation fiber
De-MUX	Demultiplexer
DFB	Distributive feedback
DHS	Double heterostructure
DLI	Delay line interferometer
DoS	Density of states
DP- QPSK	Dual-polarization quadrature phase-shift keying
DSF	Dispersion shifted fiber
DSO	Digital storage oscilloscope
DWDM	Dense wavelength division multiplexing
EAM	Electro-absorption modulator
ECL	External cavity laser
EDFA	Erbium-doped fiber amplifier
EIL	External-injection locking
ESA	Electrical signal analyzer
EVM	Error-vector magnitude
FEC	Forward error correction
FBG	Fiber Bragg grating
FP	Fabry-Perot
FSO	Free-space-optics
FSR	Free spectral range
FTTX	Fiber to the X
GS	Ground state
IoT	Internet of things
ITU	International Telecommunication Union
LD	Laser diode
LO	Local oscillator
MBE	Molecular beam epitaxy
ML	Mode-locked
MLL	Mode-locked laser
MMW	Millimeter-wave
MZM	Mach–Zehnder modulator
NG-PON	Next-generation passive optical networks
OBPF	Optical bandpass filter
OFDM	Orthogonal frequency division multiplexing
OIL	Optical injection locking
OLT	Optical line terminal
OMA	Optical modulation analyzer
ONU	Optical network unit

OOK	On-off Keying
OpEx	Operational expenditure
OSNR	Optical signal-to-noise ratio
OTDM	Optical time-division multiplexing
PAM	Pulse amplitude modulation
PBC	Polarization beam combiner
PDM	Polarization division multiplexing
PON	Passive optical network
PRBS	Pseudo random bit sequence
QAM	Quadrature amplitude modulation
Qdash	Quantum dash
Qdash LD	Quantum dash laser diode
Qdash MLL	Quantum dash mode locked laser
Qdot	Quantum dot
QPSK	Quadrature phase-shift keying
Qwell	Quantum well
Qwire	Quantum wire
RAU	Remote access unit
RF	Radio-frequency
RIN	Relative intensity noise
RoF	Radio-over-fiber
RRH	Remote radio head unit
RSOA	Reflective semiconductor optical amplifier
RTO	Real-time oscilloscope
RZ	Return to zero
SIL	Self-injection locking
SMF	Single-mode fiber
SMSR	Side mode suppression ratio
SOA	Semiconductor optical amplifier
THz	Terahertz
TIA	Trans-impedance amplifier
VoIP	Voice over Internet Protocol
WDM	Wavelength division multiplexing
WL	Wireless
WSS	Wavelength selective switch

VII. CONCLUSION

In summary, we reviewed the current advances of deploying InAs/InP Qdash broadband LDs, operating in the C- and mid L-band wavelength region in various convergent optical communications networks. The inherent ML feature of this new class of device enabled addressing green communication networks by potentially replacing several light sources with a single source in WDM networks with demonstrated 11 - 12 Tb/s aggregate data rates with PAM-4 as well as higher-order 32-QAM modulation schemes. Moreover, the deployment of optical injection locking and demonstration of 192 Gb/s data capacity in the challenging 1610 nm window substantiate the merits offered by Qdash LDs to be a potential candidate in next-generation access networks. The possibility of extending the operating window beyond the bandwidth-hungry 1550 nm telecommunication window is optimistic, thanks to the excellent long-wavelength tuning properties of InAs/InP Qdash active region, enabling demonstrated lasing emission covering C- to U-bands. Lastly, generation of high-quality MMW beat-tones from 25 to > 100 GHz, with RF linewidth in sub kHz range and extremely low phase noise floor, demonstrates this optical source's excellent performance characteristics, thus potentially realizing SMF-WL and SMF-FSO-WL convergence WDM networks for 5G access networks and beyond.

ACKNOWLEDGMENT

The author thanks Dr. Emad Alkhazraji for the help in proofreading the manuscript and providing feedback. He also thanks to the group members and collaborators for their continuous support.

REFERENCES

[1] D. Nesset, "PON roadmap," *J. Opt. Commun. Netw.*, vol. 9, no. 1, p. A71, Jan. 2017, doi: 10.1364/JOCN.9.000A71.

[2] W. P. Huang, X. Li, C. Q. Xu, X. Hong, C. Xu, and W. Liang, "Optical transceivers for fiber-to-the-premises applications: System requirements and enabling technologies," *J. Lightw. Technol.*, vol. 25, no. 1, pp. 11–27, Jan. 2007, doi: 10.1109/JLT.2006.888482.

[3] *Cisco Annual Internet Report (2018-2023) White Paper*, Cisco, San Jose, CA, USA, 2020.

[4] *Cisco Visual Networking Index: Global Mobile Data Traffic Forecast Update*, Cisco, San Jose, CA, USA, 2019.

[5] N. Cvijetic, D. Qian, and J. Hu, "100 Gb/s optical access based on optical orthogonal frequency-division multiplexing," *IEEE Commun. Mag.*, vol. 48, no. 7, pp. 70–77, Jul. 2010, doi: 10.1109/MCOM.2010.5496880.

[6] J.-I. Kani, F. Bourgart, A. Cui, A. Rafel, M. Campbell, R. Davey, and S. Rodrigues, "Next-generation PON—Part I: Technology roadmap and general requirements," *IEEE Commun. Mag.*, vol. 47, no. 11, pp. 43–49, Nov. 2009, doi: 10.1109/MCOM.2009.5307465.

[7] G. Liu, Z. Lu, J. Liu, Y. Mao, M. Vachon, C. Song, P. Barrios, and P. Poole, "Passively mode-locked quantum dash laser with an aggregate 5.376 Tbit/s PAM-4 transmission capacity," *Opt. Exp.*, vol. 28, no. 4, pp. 4587–4593, Feb. 2020, doi: 10.1364/OE.386266.

[8] Z. Lu, *Quantum-Dot Coherent Comb Lasers for Terabit Optical Networking Systems (SPIE OPTO)*. Bellingham, WA, USA: SPIE, 2019.

[9] M. A. Shemis, A. M. Ragheb, M. T. A. Khan, H. A. Fathallah, S. Alshebeili, K. K. Qureshi, and M. Z. M. Khan, "L-band quantum-dash self-injection locked multiwavelength laser source for future WDM access networks," *IEEE Photon. J.*, vol. 9, no. 5, pp. 1–7, Oct. 2017, doi: 10.1109/JPHOT.2017.2733162.

[10] M. Rahim, K. Zeb, Z. Lu, G. Pakulski, J. Liu, P. Poole, C. Song, P. Barrios, W. Jiang, and X. Zhang, "Monolithic InAs/InP quantum dash dual-wavelength DFB laser with ultra-low noise common cavity modes for millimeter-wave applications," *Opt. Exp.*, vol. 27, no. 24, pp. 35368–35375, Nov. 2019, doi: 10.1364/OE.27.035368.

[11] A. Gupta and R. K. Jha, "A survey of 5G network: Architecture and emerging technologies," *IEEE Access*, vol. 3, pp. 1206–1232, 2014, doi: 10.1109/ACCESS.2015.2461602.

[12] L. Vallejo, M. Komanec, B. Ortega, J. Bohata, D.-N. Nguyen, S. Zvanovec, and V. Almenar, "Impact of thermal-induced turbulent distribution along FSO link on transmission of photonically generated mmW signals in the frequency range 26–40 GHz," *IEEE Photon. J.*, vol. 12, no. 1, pp. 1–9, Feb. 2020, doi: 10.1109/JPHOT.2019.2959227.

[13] E. Alkhazraji, A. Ragheb, Q. Tareq, M. A. Esmail, S. Alshebeili, and M. Z. M. Khan, "Devices and technologies for Tbits^{-1} communication and beyond," in *Proc. Digit. Encyclopedia Appl. Phys.*, 2003, pp. 1–36.

[14] J. J. Coleman, J. D. Young, and A. Garg, "Semiconductor quantum dot lasers: A tutorial," *J. Lightw. Technol.*, vol. 29, no. 4, pp. 499–510, Feb. 2011, doi: 10.1109/JLT.2010.2098849.

[15] R. P. Mirin, J. P. Ibbetson, K. Nishi, A. C. Gossard, and J. E. Bowers, "1.3 μm photoluminescence from InGaAs quantum dots on GaAs," *Appl. Phys. Lett.*, vol. 67, no. 25, pp. 3795–3797, Dec. 1995, doi: 10.1063/1.115386.

[16] J. Wu and P. Jin, "Self-assembly of InAs quantum dots on GaAs(001) by molecular beam epitaxy," *Frontiers Phys.*, vol. 10, no. 1, pp. 7–58, Feb. 2015, doi: 10.1007/s11467-014-0422-4.

[17] M. Geller, "Investigation of carrier dynamics in self-organized quantum dots for memory devices," Ph.D. dissertation, Tech. Univ. Berlin, Berlin, Germany, 2007.

[18] D. Fuster, B. Alén, L. González, Y. González, J. Martínez-Pastor, M. González, and J. M. García, "Isolated self-assembled InAs/InP(001) quantum wires obtained by controlling the growth front evolution," *Nanotechnology*, vol. 18, no. 3, Jan. 2007, Art. no. 035604, doi: 10.1088/0957-4484/18/3/035604.

[19] K. Akahane, A. Matsumoto, T. Umezawa, and N. Yamamoto, "Fabrication of In(P)As quantum dots by interdiffusion of p and as on InP(311)B substrate," *Crystals*, vol. 10, no. 2, p. 90, Feb. 2020. [Online]. Available: https://www.mdpi.com/2073-4352/10/2/90

[20] M. Z. M. Khan, T. K. Ng, and B. S. Ooi, "Self-assembled InAs/InP quantum dots and quantum dashes: Material structures and devices," *Prog. Quantum Electron.*, vol. 38, no. 6, pp. 237–313, Nov. 2014, doi: 10.1016/j.pquantelec.2014.11.001.

[21] H. Dery, E. Benisty, A. Epstein, R. Alizon, V. Mikhelashvili, G. Eisenstein, R. Schwertberger, D. Gold, J. P. Reithmaier, and A. Forchel, "On the nature of quantum dash structures," *J. Appl. Phys.*, vol. 95, no. 11, pp. 6103–6111, Jun. 2004, doi: 10.1063/1.1715135.

[22] F.-J. Wang, F. Ren, S.-M. Liu, N. Zhuo, S.-Q. Zhai, J.-Q. Liu, F.-Q. Liu, and Z.-G. Wang, "Normal incident long wave infrared quantum dash quantum cascade photodetector," *Nanosc. Res. Lett.*, vol. 11, no. 1, p. 392, Dec. 2016, doi: 10.1186/s11671-016-1611-6.

[23] C. J. Gilfert, "High-speed semiconductor lasers based on low-dimensional active materials for optical telecommunication," Ph.D. dissertation, Univ. Kassel, Kassel, Germany, 2012.

[24] F. I. Zubov, S. P. Gladii, Y. M. Shernyakov, M. V. Maximov, E. S. Semenova, I. V. Kulkova, K. Yvind, and A. E. Zhukov, "1.5 μm InAs/InGaAsP/InP quantum dot laser with improved temperature stability," *J. Phys., Conf. Ser.*, vol. 741, Aug. 2016, Art. no. 012109, doi: 10.1088/1742-6596/741/1/012109.

[25] R. Wang, A. Stintz, P. Varangis, T. Newell, H. Li, K. Malloy, and L. F. Lester, "Room-temperature operation of InAs quantum-dash lasers on InP [001]," *IEEE Photon. Technol. Lett.*, vol. 13, no. 8, pp. 767–769, Aug. 2001, doi: 10.1109/68.935797.

[26] R. Schwertberger, D. Gold, J. P. Reithmaier, and A. Forchel, "Long-wavelength InP-based quantum-dash lasers," *IEEE Photon. Technol. Lett.*, vol. 14, no. 6, pp. 735–737, Jun. 2002, doi: 10.1109/LPT.2002.1003076.

[27] T. Rotter, A. Stintz, and K. Malloy, "InP based quantum dash lasers with 2μm wavelength," *IEE Proc.-Optoelectron.*, vol. 150, no. 4, pp. 318–321, 2003.

[28] S. Deubert, A. Somers, W. Kaiser, R. Schwertberger, J. P. Reithmaier, and A. Forchel, "InP-based quantum dash lasers for wide gain bandwidth applications," *J. Cryst. Growth*, vol. 278, nos. 1–4, pp. 346–350, May 2005, doi: 10.1016/j.jcrysgro.2005.01.041.

[29] A. Somers, W. Kaiser, J. P. Reithmaier, and A. Forchel, "InP-based quantum dash lasers for broadband optical amplification and gas sensing applications," in *Proc. Int. Conf. Indium Phosph. Rel. Mater.*, May 2005, pp. 56–59, doi: 10.1109/ICIPRM.2005.1517418.

[30] M. Z. M. Khan, T. K. Ng, C.-S. Lee, P. Bhattacharya, and B. S. Ooi, "Investigation of chirped InAs/InGaAlAs/InP quantum dash lasers as broadband emitters," *IEEE J. Quantum Electron.*, vol. 50, no. 2, pp. 51–61, Feb. 2014.

[31] H. S. Djie, C. L. Tan, B. S. Ooi, J. C. M. Hwang, X.-M. Fang, Y. Wu, J. M. Fastenau, W. K. Liu, G. T. Dang, and W. H. Chang, "Ultrabroad stimulated emission from quantum-dash laser," *Appl. Phys. Lett.*, vol. 91, no. 11, Sep. 2007, Art. no. 111116, doi: 10.1063/1.2784969.

[32] C. L. Tan, H. S. Djie, Y. Wang, C. E. Dimas, V. Hongpinyo, Y. H. Ding, and B. S. Ooi, "Wavelength tuning and emission width widening of ultrabroad quantum dash interband laser," *Appl. Phys. Lett.*, vol. 93, no. 11, Sep. 2008, Art. no. 111101, doi: 10.1063/1.2981578.

[33] A. E. Zhukov, M. V. Maksimov, and A. R. Kovsh, "Device characteristics of long-wavelength lasers based on self-organized quantum dots," *Semiconductors*, vol. 46, no. 10, pp. 1225–1250, Oct. 2012.

[34] C. Gosset, K. Merghem, A. Martinez, G. Moreau, G. Patriarche, G. Aubin, A. Ramdane, J. Landreau, and F. Lelarge, "Subpicosecond pulse generation at 134GHz using a quantum-dash-based Fabry–Perot laser emitting at 1.56μm," *Appl. Phys. Lett.*, vol. 88, no. 24, Jun. 2006, Art. no. 241105, doi: 10.1063/1.2213007.

[35] K. Merghem, R. Rosales, S. Azouigui, A. Akrout, A. Martinez, F. Lelarge, G.-H. Duan, G. Aubin, and A. Ramdane, "Low noise performance of passively mode locked quantum-dash-based lasers under external optical feedback," *Appl. Phys. Lett.*, vol. 95, no. 13, Sep. 2009, Art. no. 131111, doi: 10.1063/1.3238324.

[36] M. Dontabactouny, C. Rosenberg, E. Semenova, D. Larsson, K. Yvind, R. Piron, F. Grillot, O. Dehaese, N. Chevalier, and S. Loualiche, *10-GHz 1.59-μm Quantum Dash Passively Mode-Locked Two-Section Lasers (SPIE Photonics Europe)*. Bellingham, WA, USA: SPIE, 2010.

[37] R. Rosales, S. Murdoch, R. Watts, K. Merghem, A. Martinez, F. Lelarge, A. Accard, L. Barry, and A. Ramdane, "High performance mode locking characteristics of single section quantum dash lasers," *Opt. Exp.*, vol. 20, no. 8, pp. 8649–8657, 2012, doi: 10.1364/OE.20.008649.

[38] R. Rosales, K. Merghem, A. Martinez, A. Akrout, J.-P. Tourrenc, A. Accard, F. Lelarge, and A. Ramdane, "InAs/InP quantum-dot passively mode-locked lasers for 1.55-μm applications," *IEEE J. Sel. Topics Quantum Electron.*, vol. 17, no. 5, pp. 1292–1301, Sep. 2011, doi: 10.1109/JSTQE.2011.2116772.

[39] K. Merghem, A. Akrout, A. Martinez, G. Aubin, A. Ramdane, F. Lelarge, and G.-H. Duan, "Pulse generation at 346 GHz using a passively mode locked quantum-dash-based laser at 1.55 μm," *Appl. Phys. Lett.*, vol. 94, no. 2, Jan. 2009, Art. no. 021107, doi: 10.1063/1.3070544.

[40] J. C. Norman, D. Jung, Y. Wan, and J. E. Bowers, "Perspective: The future of quantum dot photonic integrated circuits," *APL Photon.*, vol. 3, no. 3, Mar. 2018, Art. no. 030901, doi: 10.1063/1.5021345.

[41] M. Z. M. Khan, E. A. Alkhazraji, M. T. A. Khan, T. K. Ng, and B. S. Ooi, "InAs/InP quantum-dash lasers," in *Nanoscale Semiconductor Lasers*, C. Tong C. Jagadish Eds. Amsterdam, The Netherlands: Elsevier, 2019, pp. 109–138.

[42] M. Z. M. Khan, E. Alkhazraji, A. M. Ragheb, M. A. Esmail, Q. Tareq, H. A. Fathallah, K. K. Qureshi, and S. Alshebeili, "Injection-locked quantum-dash laser in far L-band 192 Gbit/s DWDM transmission," *IEEE Photon. J.*, vol. 12, no. 5, Oct. 2020, Art. no. 1504211, doi: 10.1109/JPHOT.2020.3029026.

[43] E. Alkhazraji, A. Ragheb, M. Esmail, H. Fathallah, S. Alshebeili, K. Qureshi, and M. Z. M. Khan, "Three-channel multiplexed communication over mid L-band InAs/InP quantum dash laser," in *Proc. IEEE Photon. Conf. (IPC)*, Sep./Oct. 2020, pp. 1–2, doi: 10.1109/IPC47351.2020.9252459.

[44] Q. Tareq, A. M. Ragheb, E. Alkhazraji, M. A. Esmail, S. Alshebeili, and M. Z. M. Khan, "Hybrid 28 GHz MMW over fiber-wireless QPSK transmission system based on mid L-band external injection-locked quantum-dash laser comb source," *Opt. Fiber Technol.*, vol. 64, Jul. 2021, Art. no. 102553, doi: 10.1016/j.yofte.2021.102553.

[45] A. M. Ragheb, Q. Tareq, E. Alkhazraji, M. A. Esmail, S. Alshebeili, and M. Z. M. Khan, "Extended L-band InAs/InP quantum-dash laser in millimeter-wave applications," *Photonics*, vol. 8, no. 5, p. 167, May 2021. [Online]. Available: https://www.mdpi.com/2304-6732/8/5/167

[46] A. Akrout, A. Shen, F. Van Dijk, O. Legouezigou, F. Pommereau, F. Lelarge, A. Ramdane, and G. H. Duan, "Error-free transmission of 8 WDM channels at 10 Gbit/s using comb generation in a quantum dash based mode-locked laser," in *Proc. 34th Eur. Conf. Opt. Commun.*, Sep. 2008, pp. 1–2, doi: 10.1109/ECOC.2008.4729565.

[47] A. Akrout, A. Shen, R. Brenot, F. Van Dijk, O. Legouezigou, F. Pommereau, F. Lelarge, A. Ramdane, and G.-H. Duan, "Separate error-free transmission of eight channels at 10 Gb/s using comb generation in a quantum-dash-based mode-locked laser," *IEEE Photon. Technol. Lett.*, vol. 21, no. 23, pp. 1746–1748, Dec. 1, 2009, doi: 10.1109/LPT.2009.2032243.

[48] Y. M'Sallem, Q. Le, L. Bramerie, Q.-T. Nguyen, E. Borgne, P. Besnard, S. LaRochelle, L. Rusch, and J.-C. Simon, "Quantum-dash mode-locked laser source for wavelength-tunable 56 Gbit/s DQPSK," in *Proc. 36th Eur. Conf. Exhib. Opt. Commun.*, Sep. 2010, pp. 1–3, doi: 10.1109/ECOC.2010.5621590.

[49] Y. Ben M'Sallem, Q. T. Le, L. Bramerie, Q.-T. Nguyen, E. Borgne, P. B esnard, A. Shen, F. Lelarge, S. LaRochelle, L. A. Rusch, and J.-C. Simon, "Quantum-dash mode-locked laser as a source for 56-Gb/s DQPSK modulation in WDM multicast applications," *IEEE Photon. Technol. Lett.*, vol. 23, no. 7, pp. 453–455, Apr. 1, 2011, doi: 10.1109/LPT.2011.2106116.

[50] M. C. E. Silva, L. Bramerie, M. Gay, S. Lobo, M. Joindot, and J. C. Simon, "4×170 Gbit/s DWDM/OTDM transmission using only one quantum dash Fabry Perot mode-locked laser," in *36th Eur. Conf. Exhib. Opt. Commun.*, Sep. 2010, pp. 1–3, doi: 10.1109/ECOC.2010.5621270.

[51] M. Gay, A. O'Hare, L. Bramerie, Z. Hao, S. Fresnel, C. Peucheret, P. Besnard, S. Joshi, S. Barbet, and F. Lelarge, "Single quantum dash mode-locked laser as a comb-generator in four-channel 112 Gbit/s WDM transmission," in *Proc. Opt. Fiber Commun. Conf.*, San Francisco, CA, USA, 2014, p. Tu2H.5. [Online]. Available: http://www.osapublishing.org/abstract.cfm?URI=OFC-2014-Tu2H.5

[52] J. Pfeifle, I. Shkarban, S. Wolf, J. Kemal, C. Weimann, W. Hartmann, N. Chimot, S. Joshi, K. Merghem, A. Martinez, and M. Weber, "Coherent terabit communications using a quantum-dash mode-locked laser and self-homodyne detection," in *Proc. Opt. Fiber Commun. Conf.*, Los Angeles, CA, USA, Oct. 2015, p. W2A.19. [Online]. Available: http://www.osapublishing.org/abstract.cfm?URI=OFC-2015-W2A.19

[53] V. Vujicic, C. Calò, R. Watts, F. Lelarge, C. Browning, K. Merghem, A. Martinez, A. Ramdane, and L. Barry, "Quantum dash passively mode-locked lasers for Tbit/s data interconnects," in *Proc. Opt. Fiber Commun. Conf.*, Los Angeles, CA, USA, Oct. 2015, p. Tu3I.4. [Online]. Available: http://www.osapublishing.org/abstract.cfm?URI=OFC-2015-Tu3I.4

[54] R. Watts, R. Rosales, F. Lelarge, A. Ramdane, and L. Barry, "Mode coherence measurements across a 1.5 THz spectral bandwidth of a passively mode-locked quantum dash laser," *Opt. Lett.*, vol. 37, no. 9, pp. 1499–1501, May 2012, doi: 10.1364/OL.37.001499.

[55] V. Vujicic, C. Calo, R. Watts, F. Lelarge, C. Browning, K. Merghem, A. Martinez, A. Ramdane, and L. Barry, "Quantum dash mode-locked lasers for data centre applications," *IEEE J. Sel. Topics Quantum Electron.*, vol. 21, no. 6, pp. 53–60, Oct. 2015, doi: 10.1109/JSTQE.2015.2487884.

[56] V. Vujicic, A. Anthur, V. Panapakkam, R. Zhou, Q. Gaimard, K. Merghem, F. Lelarge, A. Ramdane, and L. Barry, "Tbit/s optical interconnects based on low linewidth quantum-dash lasers and coherent detection," in *Proc. Conf. Lasers Electro-Opt.*, San Jose, CA, USA, Jun. 2016, p. SF2F.4. [Online]. Available: http://www.osapublishing.org/abstract.cfm?URI=CLEO_SI-2016-SF2F.4

[57] P. Marin-Palomo, J. Kemal, P. Trocha, S. Wolf, K. Merghem, F. Lelarge, A. Ramdane, W. Freude, S. Randel, and C. Koos, "Comb-based WDM transmission at 10 Tbit/s using a DC-driven quantum-dash mode-locked laser diode," *Opt. Exp.*, vol. 27, no. 22, pp. 31110–31129, Oct. 2019, doi: 10.1364/OE.27.031110.

[58] P. Marin, J. Pfeifle, J. Kemal, S. Wolf, K. Vijayan, N. Chimot, A. Martinez, A. Ramdane, F. Lelarge, W. Freude, and C. Koos, "8.32 Tbit/s coherent transmission using a quantum-dash mode-locked laser diode," in *Proc. Conf. Lasers Electro-Opt.*, San Jose, CA, USA, Jun. 2016, p. STh1F.1. [Online]. Available: http://www.osapublishing.org/abstract.cfm?URI=CLEO_SI-2016-STh1F.1

[59] J. Kemal, P. Marin-Palomo, V. Panapakkam, P. Trocha, S. Wolf, K. Merghem, F. Lelarge, A. Ramdane, S. Randel, W. Freude, and C. Koos, "Coherent WDM transmission using quantum-dash mode-locked laser diodes as multi-wavelength source and local oscillator," *Opt. Exp.*, vol. 27, no. 22, pp. 31164–31175, Oct. 2019, doi: 10.1364/OE.27.031164.

[60] J. Kemal, P. Marin-Palomo, V. Panapakkam, P. Trocha, S. Wolf, K. Merghem, F. Lelarge, A. Ramdane, S. Randel, W. Freude, and C. Koos, "WDM transmission using quantum-dash mode-locked laser diodes as multi-wavelength source and local oscillator,"in *Proc. Opt. Fiber Commun. Conf.*, Los Angeles, CA, USA, Mar. 2017, p. Th3F.6. [Online]. Available: http://www.osapublishing.org/abstract.cfm?URI=OFC-2017-Th3F.6

[61] Z. Lu, J. Liu, P. J. Poole, Y. Mao, J. Weber, G. Liu, and P. Barrios, "InAs/InP quantum dash semiconductor coherent comb lasers and their applications in optical networks," *J. Lightw. Technol.*, vol. 39, no. 12, pp. 3751–3760, Jun. 15, 2021, doi: 10.1109/JLT.2020.3043284.

[62] V. Vujicic, A. Anthur, A. Saljoghei, V. Panapakkam, R. Zhou, Q. Gaimard, K. Merghem, F. Lelarge, A. Ramdane, and L. Barry, "Mitigation of relative intensity noise of quantum dash mode-locked lasers for PAM4 based optical interconnects using encoding techniques," *Opt. Exp.*, vol. 25, no. 1, pp. 20–29, Jan. 2017, doi: 10.1364/OE.25.000020.

[63] M. Olmedo, T. Zuo, J. Jensen, Q. Zhong, X. Xu, S. Popov, and I. Monroy, "Multiband carrierless amplitude phase modulation for high capacity optical data links," *J. Lightw. Technol.*, vol. 32, no. 4, pp. 798–804, Feb. 15, 2014, doi: 10.1364/OE.25.000020.

[64] Z. Lu, J. Liu, Y. Mao, K. Zeb, G. Liu, P. Poole, J. Weber, M. Rahim, G. Pakulski, C. Song, and M. Vachon, "Quantum dash multi-wavelength lasers for Tbit/s coherent communications and 5G wireless networks," *J. Eur. Opt. Soc.-Rapid*, vol. 17, no. 1, p. 9, Jun. 2021, doi: 10.1186/s41476-021-00156-9.

[65] G. Liu, Z. Lu, J. Liu, Y. Mao, M. Vachon, C. Song, and P. Poole, "A passively mode-locked quantum dot laser with 10.8 Tbit/s transmission over 100-km SSMF," in *Proc. Opt. Fiber Commun. Conf. (OFC)*, San Diego, CA, USA, Mar. 2020, p. W2A.2. [Online]. Available: http://www.osapublishing.org/abstract.cfm?URI=OFC-2020-W2A.2

[66] Z. Lu, J. Liu, L. Mao, C.-Y. Song, J. Weber, and P. Poole, *12.032 Tbit/s Coherent Transmission Using An Ultra-Narrow Linewidth Qantum Dot 34.46-GHz C-Band Coherent Comb Laser*. Bellingham, WA, USA: SPIE, 2019.

[67] C. Browning, T. Verolet, Y. Lin, G. Aubin, F. Lelarge, A. Ramdane, and L. Barry, "56 Gb/s/λ over 1.3 THz frequency range and 400 G DWDM PAM-4 transmission with a single quantum dash mode-locked laser source," *Opt. Exp.*, vol. 28, no. 15, pp. 22443–22449, Jul. 2020, doi: 10.1364/OE.397315.

[68] J. Kemal, P. Marin-Palomo, K. Merghem, G. Aubin, C. Calo, R. Brenot, F. Lelarge, A. Ramdane, S. Randel, W. Freude, and C. Koos, "32 QAM WDM transmission using a quantum-dash passively mode-locked laser with resonant feedback," in *Proc. Opt. Fiber Commun. Conf. Exhib. (OFC)*, Jun. 2017, pp. 1–3.

[69] J. Kemal, P. Marin-Palomo, K. Merghem, G. Aubin, F. Lelarge, A. Ramdane, S. Randel, W. Freude, and C. Koos, "32 QAM WDM transmission at 12 Tbit/s using a quantum-dash mode-locked laser diode (QD-MLLD) with external-cavity feedback," *Opt. Exp.*, vol. 28, no. 16, pp. 23594–23608, Aug. 2020, doi: 10.1364/OE.392007.

[70] G. C. Mandal, R. Mukherjee, B. Das, and A. S. Patra, "A full-duplex WDM hybrid fiber-wired/fiber-wireless/fiber-VLC/fiber-IVLC transmission system based on a self-injection locked quantum dash laser and a RSOA," *Opt. Commun.*, vol. 427, pp. 202–208, Nov. 2018, doi: 10.1016/j.optcom.2018.06.048.

[71] M. T. A. Khan, E. Alkhazraji, A. M. Ragheb, H. Fathallah, K. K. Qureshi, S. Alshebeili, and M. Z. M. Khan, "100 Gb/s single channel transmission using injection-locked 1621 nm quantum-dash laser," *IEEE Photon. Technol. Lett.*, vol. 29, no. 6, pp. 543–546, Mar. 15, 2017, doi: 10.1109/LPT.2017.2664719.

[72] J. Chen, A. Markus, A. Fiore, U. Oesterle, R. Stanley, J. Carlin, R. Houdre, M. Ilegems, L. Lazzarini, L. Nasi, and M. Todaro, "Tuning InAs/GaAs quantum dot properties under Stranski-Krastanov growth mode for 1.3 μm applications," *ACS Photon.*, vol. 91, no. 10, pp. 6710–6716, 2002, doi: 10.1063/1.1476069.

[73] M. Khan, E. Alkhazraji, M. Shemis, A. Ragheb, H. Fathallah, S. Alshebeili, and M. Z. M. Khan, "Up to 128 Gb/s DP-QPSK transmission using injection-locked quantum-dash laser for NG-PONs," in *Proc. Asia Commun. Photon. Conf.*, Guangzhou, China, Nov. 2010, p. Su2A.49. [Online]. Available: http://www.osapublishing.org/abstract.cfm?URI=ACPC-2017-Su2A.49

[74] M. A. Shemis, E. Alkhazraji, A. M. Ragheb, M. T. A. Khan, M. Esmail, H. Fathallah, S. A. Alshebeili, and M. Z. M. Khan, "Broadly tunable self-injection locked InAs/InP quantum-dash laser based fiber/FSO/hybrid fiber-FSO communication at 1610 nm," *IEEE Photon. J.*, vol. 10, no. 2, Apr. 2018, Art. no. 7902210, doi: 10.1109/JPHOT.2018.2809566.

[75] M. A. Shemis, E. Alkhazraji, M. T. A. Khan, A. M. Ragheb, M. A. Esmail, H. Fathallah, S. Alshebeili, and M. Z. M. Khan, "Coherent free-space/fiber L-band optical communication using self-injection locked InAs/InP quantum-dash laser," in *Proc. Conf. Lasers Electro-Opt.*, 2018, pp. 1–2.

[76] M. T. A. Khan, M. A. Shemis, A. M. Ragheb, H. Fathallah, S. Alshebeili, and M. Z. M. Khan, "64 Gb/s quantum-dash laser based indoor free space optical communication," in *Proc. 26th Wireless Opt. Commun. Conf. (WOCC)*, Apr. 2017, pp. 1–4, doi: 10.1109/WOCC.2017.7928981.

[77] M. Khan, M. Shemis, A. Ragheb, M. Esmail, H. Fathallah, S. Alshebeili, and M. Z. M. Khan, "4 m/100 Gb/s optical wireless communication based on far L-band injection locked quantum-dash laser," *IEEE Photon. J.*, vol. 9, no. 2, Apr. 2017, Art. no. 7901807, doi: 10.1109/JPHOT.2017.2664340.

[78] M. Khan, M. Shemis, E. Alkhazraji, A. Ragheb, M. Esmail, H. Fathallah, S. Alshebeili, and M. Z. M. Khan, "Optical wireless communication at 100 Gb/s using L-band quantum-dash laser," in *Proc. Conf. Lasers Electro-Opt. Pacific Rim (CLEO-PR)*, Jul./Aug. 2017, pp. 1–3, doi: 10.1109/CLEOPR.2017.8118852.

[79] M. A. Shemis, A. M. Ragheb, E. Alkhazraji, M. A. Esmail, H. Fathallah, S. Alshebeili, and M. Z. M. Khan, "Self-seeded quantum-dash laser based 5 m–128 Gb/s indoor free-space optical communication," *Chin. Opt. Lett.*, vol. 15, no. 10, 2017, Art. no. 100604. [Online]. Available: http://www.osapublishing.org/col/abstract.cfm?URI=col-15-10-100604

[80] M. A. Shemis, M. T. A. Khan, E. Alkhazraji, A. M. Ragheb, M. A. Esmail, H. Fathallah, K. K. Qureshi, S. Alshebeili, and M. Z. M. Khan, "Demonstration of L-band DP-QPSK transmission over FSO and fiber channels employing InAs/InP quantum-dash laser source," *Opt. Commun.*, vol. 410, pp. 680–684, Mar. 2018, doi: 10.1016/j.optcom.2017.10.080.

[81] M. A. Shemis, E. A. Alkhazraji, M. T. A. Khan, M. A. Esmail, A. M. Ragheb, H. Fathallah, S. Alshebeili, and M. Z. M. Khan, "Self-injection locked L-band quantum-dash laser diode as a source for indoor optical wireless communication," in *Proc. Asia Commun. Photon. Conf.*, Guangzhou, China, Nov. 2011, p. M3G.5. [Online]. Available: http://www.osapublishing.org/abstract.cfm?URI=ACPC-2017-M3G.5

[82] R. Mukherjee, K. Mallick, B. Kuiri, S. Santra, B. Dutta, P. Mandal, and A. S. Patra, "PAM-4 based long-range free-space-optics communication system with self injection locked QD-LD and RS codec," *Opt. Commun.*, vol. 476, Dec. 2020, Art. no. 126304, doi: 10.1016/j.optcom.2020.126304.

[83] H. Wang, C. Cheng, C. Tsai, Y. Chi, and G. Lin, "Multi-color laser diode heterodyned 28-ghz millimeter-wave carrier encoded with DMT for 5G wireless mobile networks," *IEEE Access*, vol. 7, pp. 122697–122706, 2019, doi: 10.1109/ACCESS.2019.2938263.

[84] A. Stöhr, A. Akrout, R. Bu, B. Charbonnier, F. van Dijk, A. Enard, S. Fedderwitz, D. Jäger, M. Huchard, F. Lecoche, and J. Marti, "60 GHz radio-over-fiber technologies for broadband wireless services," *J. Opt. Netw.*, vol. 8, no. 5, pp. 471–487, May 2009, doi: 10.1364/JON.8.000471.

[85] F. Van Dijk, B. Charbonnier, S. Constant, A. Enard, S. Fedderwitz, S. Formont, I. Lealman, F. Lecoche, F. Lelarge, D. Moodie, and L. Ponnampalam, "Quantum dash mode-locked lasers for millimeter wave signal generation and transmission," in *Proc. 23rd Annu. Meeting*, Nov. 2010, pp. 187–188, doi: 10.1109/PHOTONICS.2010.5698821.

[86] A. Stöhr, S. Babiel, P. J. Cannard, B. Charbonnier, F. van Dijk, S. Fedderwitz, D. Moodie, L. Pavlovic, L. Ponnampalam, C. C. Renaud, D. Rogers, V. Rymanov, A. Seeds, A. G. Steffan, A. Umbach, and M. Weiss, "Millimeter-wave photonic components for broadband wireless systems," *IEEE Trans. Microw. Theory Techn.*, vol. 58, no. 11, pp. 3071–3082, Nov. 2010, doi: 10.1109/TMTT.2010.2077470.

[87] F. V. Dijk, A. Accard, A. Enard, O. Drisse, D. Make, and F. Lelarge, "Monolithic dual wavelength DFB lasers for narrow linewidth heterodyne beat-note generation," in *Proc. Asia–Pacific Microw. Photon. Conf. Int. Topical Meeting Microw. Photon. Jointly*, Oct. 2011, pp. 73–76, doi: 10.1109/MWP.2011.6088672.

[88] M. J. Fice, E. Rouvalis, F. van Dijk, A. Accard, F. Lelarge, C. C. Renaud, G. Carpintero, and A. J. Seeds, "146-GHz millimeter-wave radio-over-fiber photonic wireless transmission system," *Opt. Exp.*, vol. 20, no. 2, pp. 1769–1774, 2012, doi: 10.1364/OE.20.001769.

[89] Z. Lu, J. Liu, C. Song, J. Weber, Y. Mao, S. Chang, H. Ding, P. Poole, P. Barrios, D. Poitras, and S. Janz, "High performance InAs/InP quantum dot 34.462-GHz C-band coherent comb laser module," *Opt. Exp.*, vol. 26, no. 2, pp. 2160–2167, Jan. 2018, doi: 10.1364/OE.26.002160.

[90] Y. B. M'Sallem, A. Shen, F. Lelarge, F. Pommereau, D. Make, S. LaRochelle, and L. A. Rusch, "Quantum-dash mode-locked lasers for tunable wavelength conversion on a 100 GHz frequency grid," *J. Opt. Commun. Netw.*, vol. 4, no. 9, p. A69, Sep. 2012, doi: 10.1364/JOCN.4.000A69.

[91] Y. Lin, A. P. Anthur, S. P. O. Duill, V. Panapakkam, Q. Gaimard, A. Ramdane, and L. P. Barry, "Quantum dash passively mode-locked lasers for coherent wavelength conversion system," *IEEE Photon. Technol. Lett.*, vol. 30, no. 10, pp. 947–950, May 15, 2018, doi: 10.1109/LPT.2018.2818410.

[92] K. Mallick, P. Mandal, R. Mukherjee, G. C. Mandal, B. Das, and A. S. Patra, "Generation of 40 GHz/80 GHz OFDM based MMW source and the OFDM-FSO transport system based on special fine tracking technology," *Opt. Fiber Technol.*, vol. 54, Jan. 2020, Art. no. 102130, doi: 10.1016/j.yofte.2019.102130.

[93] P. Mandal, K. Mallick, S. Santra, B. Kuiri, B. Dutta, and A. S. Patra, "A bidirectional hybrid WDM-OFDM network for multiservice communication employing self-injection locked qdash laser source based on elimination of rrayleigh backscattering noise technique," *Opt. Quantum Electron.*, vol. 53, no. 5, p. 263, May 2021, doi: 10.1007/s11082-021-02948-2.

[94] K. Zeb, Z. Lu, J. Liu, M. Rahim, G. Pakulski, P. Poole, Y. Mao, C. Song, P. Barrios, W. Jiang, and X. Zhang, "Photonic generation of spectrally pure millimeter-wave signals for 5G applications," in *Proc. Int. Topical Meeting Microw. Photon. (MWP)*, Oct. 2019, pp. 1–4.

[95] Z. Lu, K. Zeb, J. Liu, E. Liu, L. Mao, P. Poole, M. Rahim, G. Pakulski, P. Barrios, W. Jiang, and D. Poitras, *Quantum Dot Semiconductor Lasers for 5G and Beyond Wireless Networks*. Bellingham, WA, USA: SPIE, 2021.

[96] K. Zeb, Z. Lu, J. Liu, Y. Mao, G. Liu, P. Poole, M. Rahim, G. Pakulski, P. Barrios, W. Jiang, and X. Zhang, "An InAs/InP quantum dash buried heterostructure mode-locked laser for high capacity fiber-wireless integrated 5G new radio fronthaul systems," *Opt. Exp.*, vol. 4, pp. 16164–16174, Apr. 2021, doi: 10.1364/OE.424504.

[97] Q. Tareq, E. Alkhazraji, A. Ragheb, M. Esmail, S. Alshebeili, and M. Z. M. Khan, "Wireless transmission of millimeter waves generated by L-band InAs/InP quantum-dash laser," in *Proc. IEEE Photon. Conf. (IPC)*, Sep./Oct. 2020, pp. 1–2, doi: 10.1109/IPC47351.2020.9252531.

[98] Q. Tareq, A. M. Ragheb, M. A. Esmail, S. A. Alshebeili, and M. Z. M. Khan, "Performance of injection-locked quantum-dash MMW source under clear and dusty weather conditions," *IEEE Photon. J.*, vol. 13, no. 3, Jun. 2021, Art. no. 1500409.

[99] M. Z. M. Khan, Q. Tareq, A. M. Ragheb, M. A. Esmail, and S. A. Alshebeili, "Bidirectional MMWoF-wireless convergence system based on a 1610 nm L-band quantum-dash laser," *Opt. Exp.*, vol. 29, no. 17, pp. 27493–27507, Aug. 2021, doi: 10.1364/OE.433414.

[100] F. Lecoche, B. Charbonnier, F. Frank, F. Van Dijk, A. Enard, F. Blache, M. Goix, F. Mallecot, and D. Moodie, "60 GHz bidirectional optical signal distribution system at 3 GBPS for wireless home network," in *Proc. Int. Topical Meeting Microw. Photon.*, 2005, pp. 1–3.

[101] R. Rosales, B. Charbonnier, K. Merghem, F. Van Dijk, F. Lelarge, A. Martinez, and A. Ramdane, "InAs/InP quantum dash based mode locked lasers for 60 GHz radio over fiber applications," in *Proc. Int. Conf. Indium Phosph. Rel. Mater.*, Aug. 2012, pp. 185–187, doi: 10.1109/ICIPRM.2012.6403353.

[102] A. Delmade, T. Verolet, C. Browning, Y. Lin, G. Aubin, F. Lelarge, A. Ramdane, and L. Barry, "Quantum dash passively mode locked laser for optical heterodyne millimeter-wave analog radio-over-fiber fronthaul systems," in *Opt. Fiber Commun. Conf. (OFC)*, San Diego, CA, USA, Mar. 2020, p. W2A.41. [Online]. Available: http://www.osapublishing.org/abstract.cfm?URI=OFC-2020-W2A.41

[103] A. Delmade, C. Browning, T. Verolet, J. Poette, A. Farhang, H. H. Elwan, R. D. Koilpillai, G. Aubin, F. Lelarge, A. Ramdane, D. Venkitesh, and L. P. Barry, "Optical heterodyne analog radio-over-fiber link for millimeter-wave wireless systems," *J. Lightw. Technol.*, vol. 39, no. 2, pp. 465–474, Jan. 15, 2021, doi: 10.1109/JLT.2020.3032923.

[104] K. Mallick, P. Mandal, B. Dutta, B. Kuiri, S. Santra, R. Mukherjee, and A. S. Patra, "Bidirectional OFDM based MMW/THzW over fiber system for next generation communication," *IEEE Photon. J.*, vol. 13, no. 4, Aug. 2021, Art. no. 7301207, doi: 10.1109/JPHOT.2021.3104943.

[105] E. Alkhazraji, A. Ragheb, Q. Tareq, M. A. Esmail, H. Fathallah, S. Alshebeili, and M. Z. M. Khan, "Hybrid dual-injection locked 1610 nm quantum-dash laser for MMW and THz applications," *Opt. Commun.*, vol. 452, pp. 355–359, Dec. 2019, doi: 10.1016/j.optcom.2019.07.062.

MOHAMMED ZAHED MUSTAFA KHAN (Senior Member, IEEE) received the B.E. degree in electronics and communication engineering from Osmania University, India, in 2001, the M.S. degree in electrical engineering from the King Fahd University of Petroleum and Minerals (KFUPM), in 2004, and the Ph.D. degree in electrical engineering from the King Abdullah University of Science and Technology (KAUST), Saudi Arabia, in 2013.

He joined the Hafr Al-Bain Community College, Saudi Arabia, in 2005, where he worked as a Lecturer with the Electrical and Electronics Engineering Technology Department, until 2009. From 2014 to 2015, he was a SABIC Postdoctoral Research Fellow with the Photonics Laboratory, KAUST. He joined the Electrical (EE) Engineering Department, KFUPM, in 2015, where he is currently an Associate Professor. He is also the Founder/Director of the Optoelectronics Research Laboratory, EE Department, KFUPM, and is an Affiliate of the Center for Communication Systems and Sensing. His prior research involved developing numerical models for integrated optical device simulation. His research interests include developing near-infrared and visible semiconductor lasers and systems for applications in optical communications.

Dr. Khan is a Senior Member of Optica (formally OSA) and a member of SPIE.